

FLOW OVER LONGITUDINAL BAR BOTTOM-RACKS

**A Thesis Submitted
In Partial Fulfilment of the Requirements
for the Degree of
MASTER OF TECHNOLOGY**

**by
SHREE KANT SHUKLA**

to the

DEPARTMENT OF CIVIL ENGINEERING

INDIAN INSTITUTE OF TECHNOLOGY, KANPUR

APRIL, 1987

TO

My Father and Late Mother

- 1 DEC 1957
CENTRAL LIBRARY

Acc. No. A 98307

187-M-SHU-FLO

98307

CERTIFICATE

15/4/87
i

This is to certify that the thesis entitled
'' FLOW OVER LONGITUDINAL BAR BOTTOM-RACKS'' submitted
by Shri Shree Kant Shukla in partial fulfilment of the
requirements for the degree of Master of Technology at
Indian Institute of Technology, Kanpur is a record of
bonafied research work carried out by him under my
supervision and guidance. The work embodied in this
thesis has not been submitted elsewhere for a degree.

Dated : April 15, 1987

K. Subramanya
Dr. K. Subramanya
Professor
Dept. of Civil Engineering
Indian Institute of Technology
KANPUR

ACKNOWLEDGEMENTS

The author wishes to record his deep sense of gratitude to Dr. K. Subramanya for suggesting the problem and supervising the study covered in this thesis. The author is deeply indebted to him for his inspiring guidance, meticulous attention, constructive criticism and above all for his untiring devotion through out the tenure of this work .

Thanks are due to Sri Suresh Kumar, T.O., Sri N. Satyanarayana, T.O., and other staff of the Hydraulics Laboratory for their help in various phases of the experimental work.

The author is highly thankful to his wife, his borthers and some of his other relatives for their constant encouragement towards higher studies.

The author would also like to thank his friends, A.K. Dixit , D.K. Singh, R.K. Pachauri, R.L. Rana, S.R. Singh and Zagde for their help at certain important moments during this work.

At the end, thanks due to all those who helped the author directly or indirectly during this work.

S. K. Shukla
(Shree Kant Shukla)

CONTENTS

	<u>Page</u>
Certificate	i
Acknowledgements	ii
List of Tables	v
List of Figures	vi
Notations	Viii
Abstract	x
 CHAPTER I Introduction	 1
1.1 Bottom-racks and their applica- tions	1
1.2 Different kinds of bottom-racks	3
1.3 Hydraulics of Longitudinal bar bottom-racks	4
1.4 The present study	6
 CHAPTER II A critical review of literature	 8
2.1 Longitudinal bar bottom-racks	8
2.2 Transverse bar bottom-racks	11
2.3 Perforated plate bottom-racks	12
2.4 Slots	14
2.5 Conclusions	16
 CHAPTER III Experiments and observations	 17
3.1 Experimental set up	17
3.2 Range of parameters	22
3.3 Observations	22
3.3.1 Subcritical approach flows	23
3.3.2 Supercritical approach flows	24
 CHAPTER IV Analysis	 30
4.1 Study of the limiting inlet depth	30
4.1.1 Subcritical approach flows	30
4.1.2 Supercritical approach flows	32
4.2 Study of the coefficient of dis- charge	34

4.2.1	Parameters	34
4.2.2	Coefficient of discharge in A1 flows	37
4.2.3	Coefficient of discharge in A3 flows	41
4.2.4	Coefficient of discharge in B1 flows	44
4.3	Prediction of the diversion ratio	47
4.3.1	Parameters	47
4.3.2	Diversion ratio in A1 flows	49
4.3.3	Diversion ratio in B1 flows	51
4.3.4	Diversion ratio in A1 flows over a slot	54
4.4	Energy loss over the rack	56
4.4.1	Introduction	56
4.4.2	Energy slope in A1 flows	59
4.4.3	Energy slope in B1 flows	62
4.4.4	Energy loss in A3 flows	66
4.5	Water surface profile calculations	67
CHAPTER V	Conclusions and Recommendations	69
5.1	Conclusions	69
5.2	Recommendations	72
	List of References	73
	Appendix I	75
	Appendix II	

LIST OF TABLES

<u>Table No.</u>	<u>Title</u>	<u>Page No.</u>
3.1	Details of flumes used in the experimental study	17
3.2	Range of parameters in the experimental study	21
3.3	Range of parameters of some Trench Weir installations	23
4.1	Range of Parameters used in the study of the energy slope	65
4.2	Range of energy loss parameters in A3 flows	66

LIST OF FIGURES

<u>Fig. No.</u>	<u>Title</u>	<u>Page No.</u>
1.1	Definition sketch	5
3.1	Schematic view of the experimental setup No.1	19
3.2	Schematic view of the experimental set up No.2	20
3.3	Classification of different types of flows over bottom-racks	25
3.4	Typical water surface profiles in subcritical approach flows	27
3.5	Typical water surface profiles for super critical approach flows	28
3.6	Observed Typical velocity profiles	29
4.1	Variation of limiting inlet depth Ratio in A1 type flows	31
4.2 and 4.3	Variation of limiting inlet depth ratio with ϵ and F_o in B1 type flows	33
A4.05	Velocity triangle of the flow over the rack	36
4.4 and 4.5	Variation of C_d with $V_o^2/2gE_o$ and D/S in A1 type flows.	38 and 40
4.6	Relation of C_d with $V_o^2/2gE_o$ and D/S in A3 type flows	42
4.7	Variation of C_d in A3 type flows	43
4.8	Relation of C_d with $V_o^2/2gE_o$ and D/S in B1 type flows	45

4.9	Variation of C_d in Bl type flows	46
4.10	Variation of diversion ratio in Al type flows	50
4.11	Variation of diversion ratio in Bl type flows	52
4.12	Relation of m with D/S	53
4.13	Variation of diversion ratio for a slot in Al type flows	55
4.14	Variation of energy loss over the rack in Al type flows	57
4.15	Variation of energy loss over the rack in Bl type flows	58
4.16	Relation of energy slope with L/y_{1e} and D/S in Al type flows	60
4.17	Variation of energy slope over the rack in Al type flows	61
4.18	Relation of energy slope with L/y_{1e} and D/S in Bl type flows	63
4.19	Variation of energy slope over the rack in Bl type flows	64

NOTATIONS

B	Width of rack = Width of flume
C_d	Coefficient of discharge through the rack $(= \frac{Q_D}{BL\sqrt{2g} E_o})$
D	Diameter of rack bars
E	Specific energy of the flow at a section
E_L	Total energy loss over the rack
F	Froude number of the flow at a section
L	Abstraction length of the rack
N	Number of bars in the rack
Q_D	Diverted flow through the rack
Q_R	Residual flow in the flume
Q_S	Total flow of the approaching stream
q_*	Diverted discharge per unit length of the rack
R_{eo}	Reynolds number of the flow at section (O)
R_{er}	Reynolds number of the flow through the rack
S	Clear spacing between rack bars
S_b	Submergence of the inlet
S_e	Energy slope along the rack
T	Temperature of water in degree centigrates
V	Mean velocity of the flow
V_r	Resultant average velocity of flow through rack
y_{1e}	Depth of flow at beginning of the rack
y_{2e}	Depth of flow at end of the rack
y_c	Critical depth of approach flow
y_{c1}	Downstream critical depth
y_o	Depth of approach flow (at section (O))
y_{1L}	Limiting inlet depth of flow
ϵ	Opening area ratio of the rack $(1-ND/B)$
ν (Nu)	Kinematic viscosity of water.

ABSTRACT

An experimental study of the hydraulic behaviour of longitudinal bar bottom-racks for different flow conditions and geometry of the rack has been carried out. The flow has been classified into five types viz, A1, A2, A3, B1 and B2, based on the approach flow condition and the effect of the tail water at the inlet. The A1, A3, and B1 flows have been studied in detail in the present work. The variation of the limiting inlet depth ratio with the opening area ratio of the rack has been determined in A1 and B1 flows and this enables one to predict whether the flow over the rack is fully submerged or not. A suitable coefficient of discharge has been defined by using a working specific energy head and the orifice type of flow. Important flow and rack parameters affecting the coefficient of discharge C_d have been identified. The flow parameter in A1 flows was found to have negligible effect on C_d , while it has considerable effect in A3 and B1 flows. The variation of the discharge diversion in a rack has also been studied with pertinent flow and rack parameters for A1 and B1 flows separately.

The energy loss was found to be substantial particularly in A1 and B1 flows, though it was negligible in A3 flows. The energy slope over the rack has been studied with prominent flow and rack parameters and approximate relationships have been obtained for evaluating the energy slope in

A1 and B1 flows. This information will be useful in realistic estimation of water ~~sur~~face profiles over a rack.

The findings of the present study provides basic data for effective and rational design of trench weirs.

CHAPTER I

INTRODUCTION

1.1 Bottom-Racks and Their Applications:

Hydraulic structures are used to utilise effectively the available water-resources. Plans for the development of water-resources demand improved performance of hydraulic structures to harness river waters. Bottom-racks, also called as bottom-intakes, are hydraulic structures used to divert the flow in open-channels. Such bottom-intakes find diverse applications in different fields of hydraulic engineering, particularly in diverting water from mountainous streams. Some of the applications of bottom intakes are listed below.

- (1) An application of bottom-intake which is becoming more popular nowadays because of the economy in its use as horizontal trash racks in the hydro-power plants located on mountainous streams. Such a structure, besides being simple in construction, eliminates the possible damage during floods to which any raised crest across the streams used for flow diversion would be susceptible.

Such bottom-intakes in the streams are also known as 'Trench Weirs'. Some of the trench weir installations in India are:

- (i) Two components of Binwa Hydroelectric project (H.P.)
2x3MW.

- (ii) Andhra Hydroelectric project (H.P.) 3x5.65MW.
- (iii) Bhaledh Nallah component of Baira-Siul Hydel Project 3x60 MW.
- (iv) Stakna Hydel project, Leh (J and K).

Detailed information on Trench Weirs are available in Ref.(2,9).

- (2) In an irrigation canal system the surface runoff may some times be let into a canal and excess flow may be disposed off at some convenient location downstream to a suitable drainage. The bottom-racks can effectively be used for this purpose.
- (3) A very common use of bottom-racks is as '' Kerb-outlets'' on the sides of main street to drain storm water into the subsurface drains. These outlets may be made up of horizontal or slightly inclined bottom racks.
- (4) Often, the bottom-racks are used as '' Skimmers '' when it is desired to reduce the volume of water to transport fish (1).
- (5) Bottom-rack can also be used in the sedimentation tanks to trap the debris in the grit chambers (11).
- (6) A bottom-intake structure designed for the use by the Government of Hong Kong to divert water from streams draining the Sai Kung Peninsula by a system of shafts and tunnels to a reservoir at high island is described in Ref.(14).

1.2 Different Kinds of Bottom-Racks:

Fig. 1.1 shows a typical definition sketch of a bottom-rack assembly. The bottom-racks can be classified into four categories on the basis of the nature of the rack as:

(i) Transverse bar bottom-racks:

In these racks the bars are placed transverse to the direction of flow. The bars may be of circular, rectangular or of any special shape to meet the specific requirement. When the width of the stream is large compared to the length of rack, the installation of these racks may sometimes prove to be uneconomical because of the requirement of too lengthy bars.

(ii) Longitudinal bar bottom-racks:

In these racks the bars are laid parallel to the direction of flow. The bars are of any convenient shape. These racks are convenient to install under field conditions, where the width of the stream is large compared to the length of the rack. All the trench weirs adopt this type of bottom-racks.

(iii) Perforated plate bottom-racks:

Such racks are generally used in process industries. These are plates having uniformly spaced or staggered circular holes.

(iv) Slots:

Slots are the limiting case of bottom-racks with all the bars removed.

Further to the above classification the bottom-racks may be horizontal or inclined with reference to approach bed level of the channel.

The present investigation is confined to the study of horizontal longitudinal bar bottom-racks with circular bars only.

1.3. Hydraulics of Longitudinal Bar Bottom-Racks:

The flow over the bottom-rack is a spatially varied flow with decreasing discharge. The performance of a bottom rack depends upon the flow characteristics such as the amount of main flow, the state of flow approaching the rack and the geometric characteristics of the rack such as it's length, width, slope and the shape, width and spacing of the rack elements.

Fig. 1.1 is a definition sketch of the flow over a horizontal longitudinal bar bottom-rack. The bars are made of circular rods of diameter D . The main variables involved in the problem are:

(a) Flow characteristics:

Rate of approach flow Q_S , rate of diverted flow through the rack Q_D , state of approach flow, depths y_0, y_{1e} and y_{2e} .

(b) Geometry of the Rack:

This includes the length L , width B of the rack, the bar diameter D . and clear spacing S between bars.

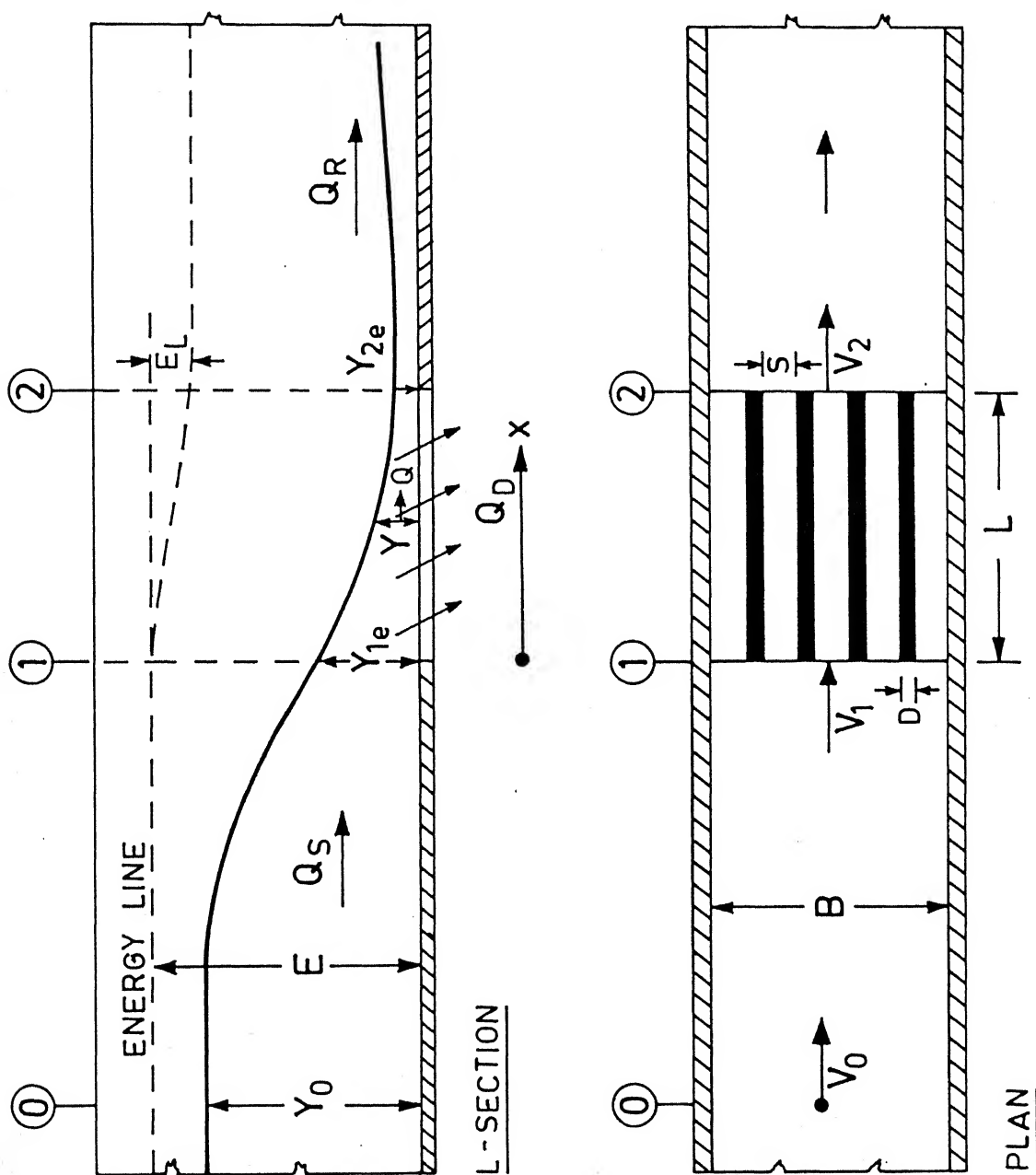


Fig. 1.1. Definition Sketch.

(c) The fluid properties:

Chiefly the dynamic viscosity μ and mass density ρ of water.

The basic hydraulic characteristics required to be predicted are:

- (i) To classify the different types of flows over the rack.
- (ii) A suitably defined coefficient of discharge C_d and it's variation.
- (iii) The diversion ratio Q_D/Q_S of the rack.
- (iv) The water-surface profile over the rack.
- (v) The energy loss over the rack.

The above information will help one to design such a bottom-intake with help of known parameters.

1.4 The Present Study:

A study of the relevant literature on the topic of bottom-racks indicated that this field has received very little attention compared to it's practical importance. The available works while meagre are essentially for the slots (4,6,11,13) and transverse bar racks (7,8,10). The case of longitudinal bar bottom-racks while being important from practical point of view, has not received due attention and the studies are limited to a few exploratory investigations (3,5,14).

Keeping in mind the unsatisfactory information available, an experimental study, to predict the hydraulic behaviour of horizontal longitudinal bar bottom-racks made up of circular bars, was designed to get maximum possible useful information within the limitations of available time. The present study includes different approach flow conditions and geometries of the rack. Some of the related works available in the literature have been compared with the data of present study. The arrangement of different topics in the thesis is as follows:

A critical review of the available literature has been presented in Chapter II. Chapter III contains the details of experiments and observations. Analysis of the data collected in the present study is given in Chapter IV. The various conclusions arising out of the present study have been collected in Chapter V. Certain recommendations for further studies on this topic are also listed in this Chapter.

Appendix I contains the basic as well as derived data of the present study. All the data are given in a convenient tabular form. In Appendix II a design procedure for a bottom-intake has been explained. A simple Fortran program has also been given for designing such a bottom-intake in practical situations where the approach flow conditions and the rate of flow to be diverted from the intake are known. A worked example also has been given by taking the data from model studies of Banu and Parai Khads of Himanchal Pradesh and results have been compared with their original recommended design.

CHAPTER II

A CRITICAL REVIEW OF LITERATURE

Flow over bottom-rack belongs to the category of spatially varied flow with decreasing discharge. Determination of the performance of a bottom-rack is a complex problem involving a large number of variables. Many investigations have been carried out with a view to evolve a proper design for a bottom-intake. Serious efforts to analyse and understand the phenomenon of flow over bottom-racks, however, have been devoted only since last three decades. Some of the important works are reviewed below:

2.1 Longitudinal Bar Bottom-Racks:

A rational approach to the problem of bottom-racks was given by Mostkow(3). His experiments were conducted on intakes having longitudinal bar bottom-racks. For the analysis, he assumed that for such bottom-racks the specific energy of the flow all over the rack remains constant and is taken as effective head causing the flow through the rack. The discharge per unit length of rack, by considering it as an orifice, was given as

$$\left(-\frac{dQ}{dx}\right) = C_1 \epsilon B \sqrt{2gE} \quad (2.1)$$

where C_1 = coefficient of discharge of longitudinal bar bottom-racks and E = constant specific energy all over rack.

The differential equation of SVF for horizontal frictionless channel will be

$$\frac{dy}{dx} = \frac{Qy(-\frac{dQ}{dx})}{gB^2y^3 - Q^2} \quad (2.2)$$

Further, the discharge Q at any section is given by

$$Q = By \sqrt{2g(E-y)} \quad (2.3)$$

substituting Eqs. (2.1) and (2.3) in (2.2) and integrating the final equation hence found, a equation for water surface profile was obtained as:

$$x = \frac{E}{C_1 E} \left(\frac{y_{1e}}{E} \sqrt{1 - \frac{y_{1e}}{E}} - \frac{y}{E} \sqrt{1 - \frac{y}{E}} \right) \quad (2.4)$$

The value of the coefficient C_1 was assumed to be constant for a particular slope of the rack. He suggested that the value of C_1 varies from 0.435, for a grade of 1 on 5, to 0.497, for a horizontal slope of the rack.

Nosedá (5) has analytically studied the characteristics of a longitudinal bar bottom-intake. His assumptions are similar to that of Mostkow, with an addition that the approach flow to the rack is critical. The discharge per unit length of the rack was defined as

$$\left(-\frac{dQ}{dx}\right) = C_n E B \sqrt{2gy} \quad (2.5)$$

where C_n = coefficient of discharge . The critical approach flow was given as

$$Q_S^2 = gB^3 y_{1e}^3 \quad (2.6)$$

The discharge diversion Q_D/Q_S from constant specific energy criteria and Eq. (2.6) is

$$\frac{Q_D}{Q_S} = 1 - \left[2 \left(\frac{3}{2} - \frac{y_{2e}}{y_{1e}} \right) \right]^{1/2} \frac{y_{2e}}{y_{1e}} \quad (2.7)$$

Eqs. (2.5) and (2.7) were combined and integrated to provide the relationship between two brink depths and length of the rack:

$$\begin{aligned} \sqrt{2} C_n \in L/y_{1e} = & \frac{3}{4\sqrt{2}} (\sin^{-1}(1/3) - \sin^{-1}(\frac{4y_{2e}}{3y_{1e}} - 1)) \\ & + \frac{3}{2} (1 - (\frac{3y_{2e}}{y_{1e}} - \frac{2y_{2e}^2}{y_{1e}^2})^{1/2}) \end{aligned} \quad (2.8)$$

Finally, the general diversion characteristics relating the diverted flow and the stream flow was derived as a plot, using:

$$(\sqrt{2} C_n \in L/y_{1e})^{-3/2} = \frac{Q_S/B}{g^{1/2} (\sqrt{2} \in C_n)^{3/2} L^{3/2}} \quad (2.9)$$

Naseda suggested that C_n is independent of stream flow Q_S and aspect ratio of the bars (D/L). Assuming C_n as 0.815 for a given rack geometry and y_{1e}, y_{2e} with the help of above Eqs. (2.7, 2.8, 2.9) a design chart as a plot of

$$\frac{Q_D/B}{g^{1/2} (\sqrt{2} \in C_n)^{3/2} L^{3/2}} \text{ Vs } \frac{Q_S/B}{g^{1/2} (\sqrt{2} \in C_n)^{3/2} L^{3/2}} \text{ has been}$$

recommended by Naseda to study the diversion characteristics.

White, et al (14) conducted model tests and compared the performance of bottom-intakes having different

length of bars, bar spacing, the transverse slope of the top surface of the bars and analysed the data on the basis of Nosedá's work. The tests were conducted on racks made of longitudinal bars with special sloping top surfaces. Racks were kept at a constant longitudinal slope of 1 vertical on 5 horizontal. In these tests the value of ϵ ranged from 0.167 to 0.333 and L/w from 6 to 10 where w = width of rack bars. This study has shown that C_n is not independent of stream flow as suggested by Nosedá. A design chart based on the model tests, as a plot of $\frac{Q_s}{BL\epsilon\sqrt{gw}}$ Vs $\frac{Q_D}{BL\epsilon\sqrt{gw}}$ valid for $6 < \frac{L}{w} < 10$; $0.167 < \epsilon < 0.333$ and critical approach flow to the rack only has been given by them. Further, regarding the shape of bars White, et al suggested that a 'no flow rejection' along the top of bars at lower stream flows can be achieved by providing the transverse top surface slope on the bars, having value between 1 in 3 to 1 in 2.

2.2 Transverse Bar Bottom-Racks:

Subramanya and Sengupta (8,10) have conducted an extensive experimental study on the flow over transverse bar bottom-racks. The racks were made of rectangular bars of width w . It was shown that Mostkow's coefficient of discharge C_1 depends upon the approach state of flow, viz whether sub-critical or supercritical and on the aspect ratio w/L of bars. When the approach flow is supercritical, C_1 varies significantly with the area factor. The coefficient C_1 decreases as the approach flow Froude number is increased and the influence

of w/L is less pronounced. The same trend appears to exist when the approach flow is subcritical, though w/L has more pronounced effect on the value of C_1 . Further, it was found that value of C_1 is large for subcritical flows than for supercritical flows. They have not studied the effect of inclination of the rack on C_1 . The assumption of constant specific energy through out the rack length, for determination of the water surface profiles, is questionable.

Rangaraju, et al (7) studied the flow over bottom-racks comprising of transverse circular bars. The experimental study was limited to subcritical approach flows only. A set of equations relating the length of the rack to hydraulic parameters and empirical relations for the contraction coefficient as well as the discharge coefficient have been proposed. It has been shown that the coefficient of contraction is mainly the function of Reynolds number of the approach flow, Froude number of the flow over rack and the opening area ratio of the rack. Further, it was shown that there is an energy loss over the rack which ranges from 20 percent to 50 percent of the initial specific energy. A method of computing the discharge through-racks and the depths at the inlet and exit has been proposed.

2.3 Perforate Plate Bottom-Racks:

An analytical and experimental study conducted by Mostkow (3), is perhaps the major work available for perforated plate bottom-racks. For the analysis, he assumed that the effective head causing the flow is equal to the

depth of flow over the rack. The outflow discharge per unit length through the rack, was presented as

$$\left(-\frac{dQ}{dx}\right) = C_2 \epsilon B \sqrt{2gy} \quad (2.10)$$

where C_2 = coefficient of discharge for perforated plate bottom-racks. The differential equation of SVF assuming the channel to be horizontal and frictionless, will be

$$\frac{dy}{dx} = \frac{Q_y \left(-\frac{dQ}{dx}\right)}{gB^2 y^3 - Q^2} \quad (2.11)$$

substituting Eqs (2.10) and (2.3) in Eq. (2.11) and integrating by using the boundary condition $y = y_{1e}$ at $X = 0$, yields the SVF profile for perforated plate bottom-racks as

$$X = \frac{E}{\epsilon C_2} \left[\frac{1}{2} \left(\cos^{-1} \sqrt{\frac{y}{E}} - \cos^{-1} \sqrt{\frac{y_{1e}}{E}} \right) + \frac{3}{2} \left(\sqrt{\frac{y_{1e}}{E} \left(1 - \frac{y_{1e}}{E}\right)} - \sqrt{\frac{y}{E} \left(1 - \frac{y}{E}\right)} \right) \right] \quad (2.12)$$

Mostkow (3) found that C_2 is constant for a particular slope of the rack and varies from 0.750, for a grade of 1 on 5, to 0.800, for a horizontal slope of the rack. Sengupta (8) has shown the variation of C_2 with F_1, ϵ and w/L for super-critical approach flows. Subramanya (10) suggested that C_2 could be expected to be given by

$$C_2 = \text{fn} (F_1, \epsilon, \lambda_1, \lambda_2) \quad (2.13)$$

where λ_1 = a hole spacing parameter and λ_2 = a hole arrangement parameter. No extensive analysis and experimental study is available regarding the variation of C_2 .

2.4 Slots:

Studies on hydraulic characteristics of bottom-slots have been reported by Venkataraman (4,11,13) and Ramamurthy (6). Venkataraman, et al (4) have conducted an analytical and experimental study of the flow with a slot spanning the entire width of the channel. Defining the coefficient of discharge through the slot C_{dv} as:

$$C_{dv} = \frac{Q_D}{BL \sqrt{2gE_1}} \quad (2.14)$$

where E_1 = specific energy of the flow at inlet. An expression for the variation of C_{dv} has been obtained as

$$C_{dv} = 0.611 \sqrt{1 - (V_1^2 / 2gE_1)} \quad (2.15)$$

The Equation 2.15 was also verified experimentally for subcritical as well supercritical approach flows. A momentum formulation for the brink depth ratio y_{1e}/y_{2e} has been proposed. The ratio Q_D/Q_S is defined as performance factor of the slot and is found to be a function of L/y_c given as:

$$\frac{Q_D}{Q_S} = 0.59 (L/y_c) + 0.04 (L/y_c)^2 \quad (2.16)$$

Venkataraman (11,13) defined another coefficient of discharge C_{dvl} as

$$C_{dvl} = \frac{Q_D}{BL \sqrt{2gy_{1e}}} \quad (2.17)$$

and observed experimentally that it is invariant with F_1 and y_{1e}/L but decreases with the increase in length L of the opening.

Ramamurthy, et al (6) based on two dimensional channel outlet model and experimental data, presented a functional relationship between the discharge coefficient C_{dr} and the velocity parameter η_1 with $\frac{L}{y_{1e}}$ as the group parameter for the floor slot discharge, as

$$C_{dr} = 0.611 + C_{1r}\eta_1^2 + C_{2r}\eta_1^4 + C_{3r}\eta_1^6 + \dots \quad (2.18)$$

for $0 < \frac{L}{y_{1e}} \leq 1.0$; $0 < \eta_1 \leq 1.0$

where $C_{1r} = -0.538 + 0.254 \left(\frac{L}{y_{1e}} \right)$; $C_{2r} = 0.058 + 0.234 \left(\frac{L}{y_{1e}} \right)$

and $C_{3r} = -0.129 - 0.489 \left(\frac{L}{y_{1e}} \right) \dots \dots (2.19)$

$$\eta_1 = \frac{1}{1 + \frac{2P_c}{F_1^2}} \quad (2.20)$$

and P_c = Pressure correction factor for curvilinear flows
= fn (L/y_c)

Venkataraman, et al (12) have conducted on experimental study including all types of bottom-racks and slot. They have shown that the assumption of constant specific energy along the rack is confirmed for subcritical approach flows for racks with small openings. In all other cases an energy decrease along the rack was noted, but no detailed study in this regard is reported.

2.5 Conclusions:

On reviewing the available literature it is observed that results of many investigations are of very limited nature. Most of them belong to the category of transverse bar bottom-racks or slots. Further, the assumption of constant specific energy all over the rack is questionable. Since the parallel bar bottom-racks are important from the point of view of practical applications, it was felt worth while to conduct an experimental study for analysing the flow over such racks including as many variable as possible.

CHAPTER III

EXPERIMENTS AND OBSERVATIONS

3.1 Experimental Set-up:

To study the hydraulic behaviour of horizontal longitudinal bar bottom-racks, experiments were carried out in the hydraulic laboratory of the Indian Institute of Technology, Kanpur. The experiments were conducted in two flumes, Flumes A and B, with details as given below:

Table 3.1 Details of Flumes Used in the Experimental Study

	Flume A	Flume B
Width	0.60 m	0.15 m
Length	9.00 m	3.00 m
Type	Non-recirculating	Partially -recirculating
Bed	Horizontal and Smooth	Horizontal and Smooth
Side Walls	Masonry Side Walls	Plexi-glas Side Walls
Cross-Section	Rectangular	Rectangular
Max. Discharge Available	95 Liters/S	18 Liters/S
Upstream Control	Sluice Gate	Sluice Gate
Downstream Control	Bottom-hinged Flap Gate	Sluice Gate

The diverted flow through the rack in flume A was passed through channel No. II and measured by a rectangular-notch fitted at its downstream end. Residual flow was passed

through channel No. III and measured by a V-Notch. The Notches were calibrated before starting the experiments. A schematic view of experimental set up No. 1 for flume A is given in Fig. 3.1 The diverted flow through the rack in flume B was measured by a 90° V-Notch and the total stream flow was measured by a calibrated venturimeter fitted in the supply pipe. For the head measurements in Notches, point gauges with least count of 0.1 mm were used. A schematic view of experimental set up No.2 for flume B is given in Fig. 3.2.

In flume A, a slot having width $B = 60$ cm and Length $L = 30$ cm, was cut at a distance of 5 meter, from the upstream gate. The rack made of circular bars could be placed in this slot. The diameter D of the bars was kept 22 mm and the bars were placed at uniform clear spacing S . Keeping $D = 22$ mm as constant and varying the spacing S , four sets of racks were prepared having D/S ratios of 1.13, 2.05, 2.90 and 5.60. Then for the same rack by using a cover plate beneath and filling the gaps by cement mortar uniformly, the length of the rack was reduced to 15 cm, to achieve $B/L = 4.0$. All the four rack sets having the D/S ratios mentioned above were also tested by making $B/L = 4.0$. With the available discharge and downstream control only supercritical approach flow could be obtained in flume A.

In flume B, a slot of width $B = 15$ cm and length $L = 7.5$ cm. was cut at a distance 2.56 meters, from the

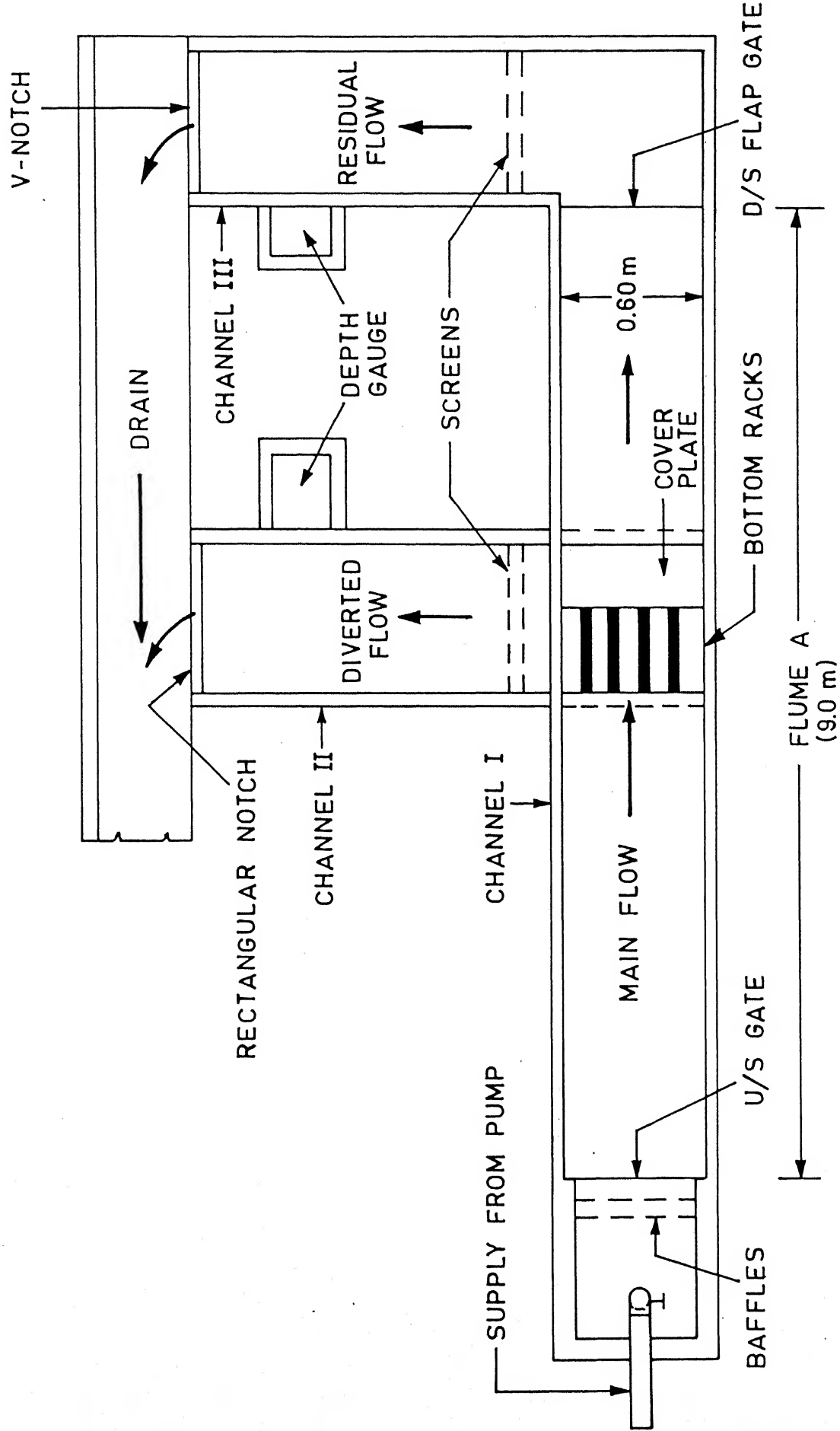


Fig. 3.1. Schematic View of the Experimental Setup No. 1.

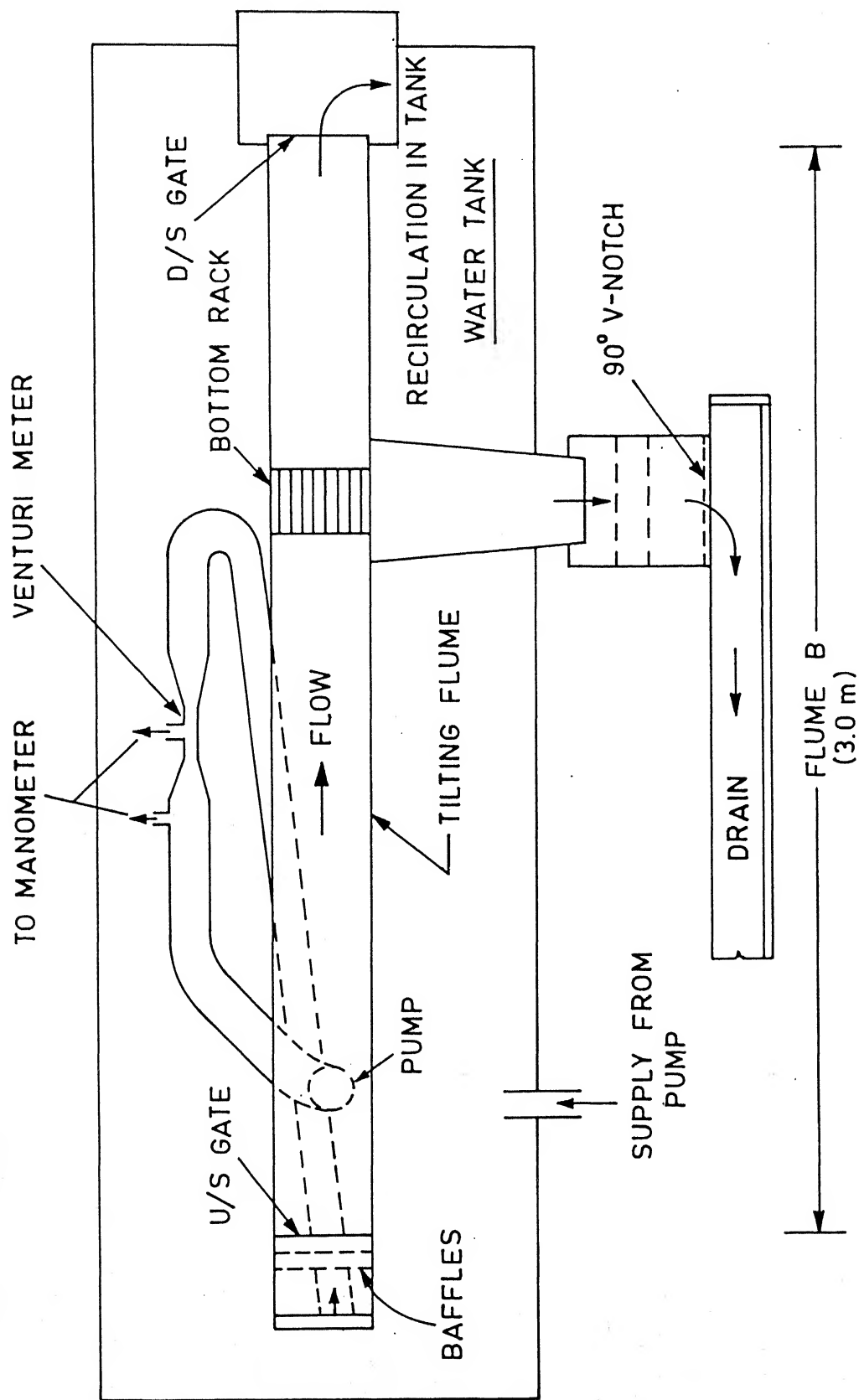


Fig. 3.2. Schematic View of the Experimental Setup No. 2.

upstream gate. Circular bars of diameter 6 mm were used for all the rack assemblies and the bars were placed at uniform clear spacing. The spacing S was changed for different rack sets to achieve four sets of D/S ratios of 1.17, 1.89, 3.33 and 5.50. With the help of small angles placed underneath the rack from both sides, the length could be reduced to 3.75 cm to achieve $B/L = 4.0$ for all the four rack sets. With the available discharge and downstream control only subcritical approach flow could be obtained in this flume. For the study of flow over a pure slot the flume B was chosen and a slot having $B=15$ cm was made. After this study, the slot length was reduced to 3.75 cm to get $B/L = 4.0$. When the whole flow was diverted within certain length of rack, this particular length was taken as L .

Table 3.2 Range of Parameters in the Experimental Study

Parameter	Range
D/S	1.13 to 5.60
ϵ	0.157 to 0.487
B/L	2.00 and 4.00
D	0.60 cm and 2.20 cm
F_o	0.200 to 5.40
R_{er}	3.5×10^3 to 3.5×10^4
R_{eo}	1×10^4 to 1.95×10^5
$V_o^2 / 2gE_o$	0.02 to 0.95

3.2 Range of Parameters:

A total of 146 runs were conducted and the range of various parameters studied are shown in Table 3.2 .

Where $F_o = \frac{V_o}{\sqrt{gy_o}}$ = froude number of approach flow at section (0) defined in Fig. 1.1.

R_{eo} = Approach flow Reynolds number at section (0)

$R_{er} = \frac{Q_D}{BLE\nu} = \text{Reynolds number of the flow through the rack.}$

ν = Kinematic viscosity of water ; and

Q_D = Diverted flow through the rack.

The present study fairly covers the usual practical ranges of parameters used in the design of Trench weirs, as can be seen from Table 3.3 where some parameters corresponding to the design data of trench weirs are given.

3.3 Observations:

For a given rack in a flume, a series of experiments were conducted starting from the smallest discharge and gradually increasing it in steps till the maximum discharge capacity of the flume was reached. In a typical experiment the centre line depth of flow along the flume at different sections were measured with a movable point guage of least count 0.1 mm. On the basis of the water surface profiles that exist over the rack and the approach flow, the flows can be grossly classified into two categories viz, subcritical and supercritical approach flows.

Table 3.3 Range of Parameters of Some Trench Weir Installations

Parameters	<u>Binwa Hydel Project (9)</u>		Andhra Hydel Project (2)
	Banu Weir	Parai Weir	
D/S	0.8333	0.8333	1.333
ϵ	0.490	0.490	0.429
B/L	7.000	3.000	26.670
D	2.5 cm	2.5 cm	4.0 cm
F_o	2.00	1.10	—*
R_{er}	5.6×10^3	2.0×10^4	1.4×10^4
$V_o^2/2gE_o$	0.670	0.370	—*

* = Data not available

3.3.1 Subcritical Approach Flow:

In the case of subcritical approach flow the depth of flow continuously decreases from upstream gate to the beginning of the rack. It is observed that the flow becomes supercritical at the inlet to the rack, hence producing a critical flow condition a little distance upstream from the inlet. The depth of flow decreases along the rack and supercritical flow exists all over it. Downstream of the rack the depth increases slightly due to friction. Depending upon the tail water condition a jump may occur downstream to the rack. This jump may shift upstream and may form even in the middle of the rack itself. So long as the inlet

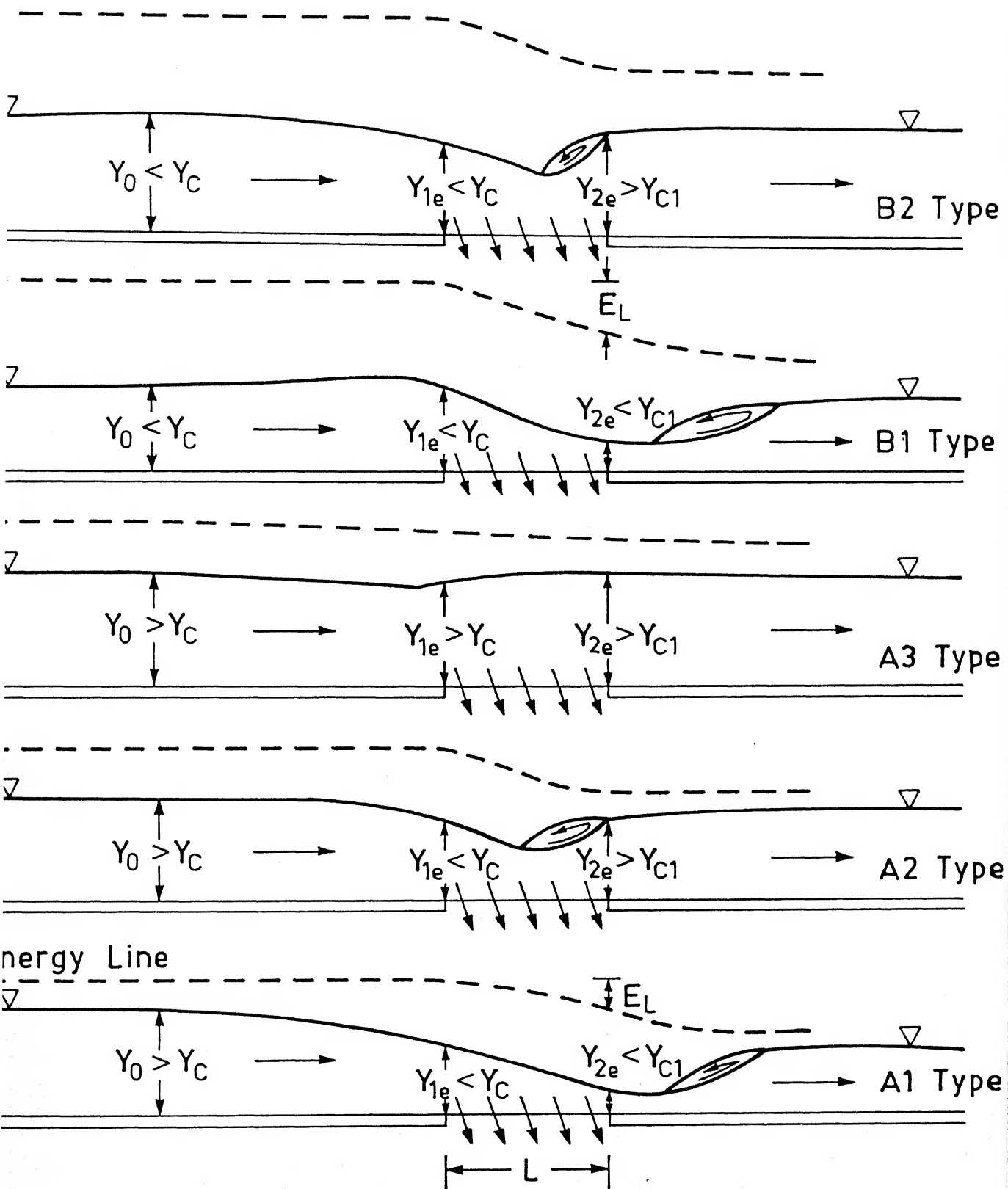
depth y_{1e} is not affected by the jump (i.e. tail water) such flows are designated as 'Free flows'. When the jump shifts further upstream the inlet becomes submerged and the flow becomes subcritical all along the channel. Thus, three types of flows could be identified in this category:

- A1 : Subcritical approach flow and super critical flow all over the rack. This is called 'subcritical approach free flow.'
- A2 : Subcritical approach and partial supercritical over the rack.
- A3 : Subcritical flow all along the channel. This is called 'Subcritical approach submerged flow'.

All the three types of flows are shown in Fig. 3.3. In this figure y_c is upstream critical depth and y_{c1} stands for downstream critical depth.

3.3.2 Super Critical Approach Flows:

In the category of supercritical approach flows it was observed that for lower Froude numbers (say $F_0=1.2$) the water surface drops from the upstream gate to the beginning of the rack. The depth of flow decreases along the rack and the flow along it will also be supercritical. After the end of the rack the depth increases slightly due to friction. The same trend is observed for all the lower Froude numbers ($R_0=1.0$ to 1.4). But when the Froude number is more than about 2.0 the depth increases from upstream gate upto about



3.3. Classification of Different Types of Flows Over Bottom-racks.

the beginning of the rack due to high channel friction and drops down at the beginning of the rack. Depending upon the downstream control, a jump may some time occur downstream of the rack and may shift upstream to produce subcritical flow in the neighbourhood of inlet in the approach channel. Also it can be observed that for Froude numbers greater than 2.0 there is lesser difference between y_{2e} and y_{1e} compared to that in the Froude number range of 1.0 to 1.4. Thus two types of flows may be clearly identified:

- B1 : Supercritical approach flow and supercritical flow all over the rack.
- B2 : Super critical approach flow and partial sub-critical over the rack.

B1 and B2 types of flows are shown in Fig. 3.3. Typical observed water surface profiles for different types of flows A1, A2 and A3 are shown in Fig. 3.4. Fig. 3.5 shows the profiles, all corresponding to B1 flows only. For a few runs the velocity profiles were also measured at certain sections of the channel. Some of the observed velocity profiles are shown in Fig. 3.6.

The present investigation is confined to the study of A1, A3 and B1 flows. The flow types A2 and B2 are beyond the scope of the present study in view of the complex flow situations. The data collected in A1, A3 and B1 flows are summarised in Appendix I.

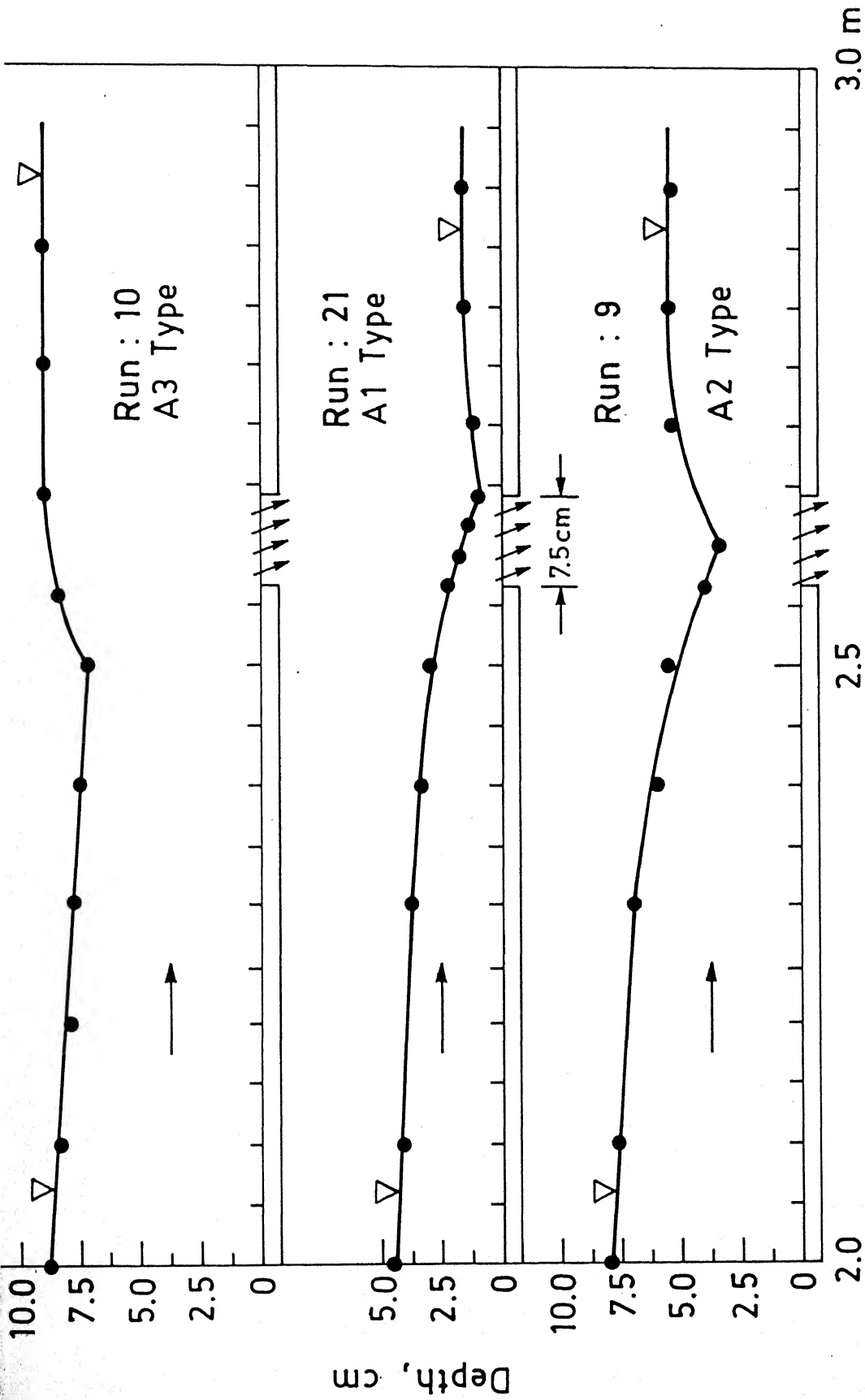


Fig. 3.4. Typical Water Surface Profiles in Subcritical Approach Flows.

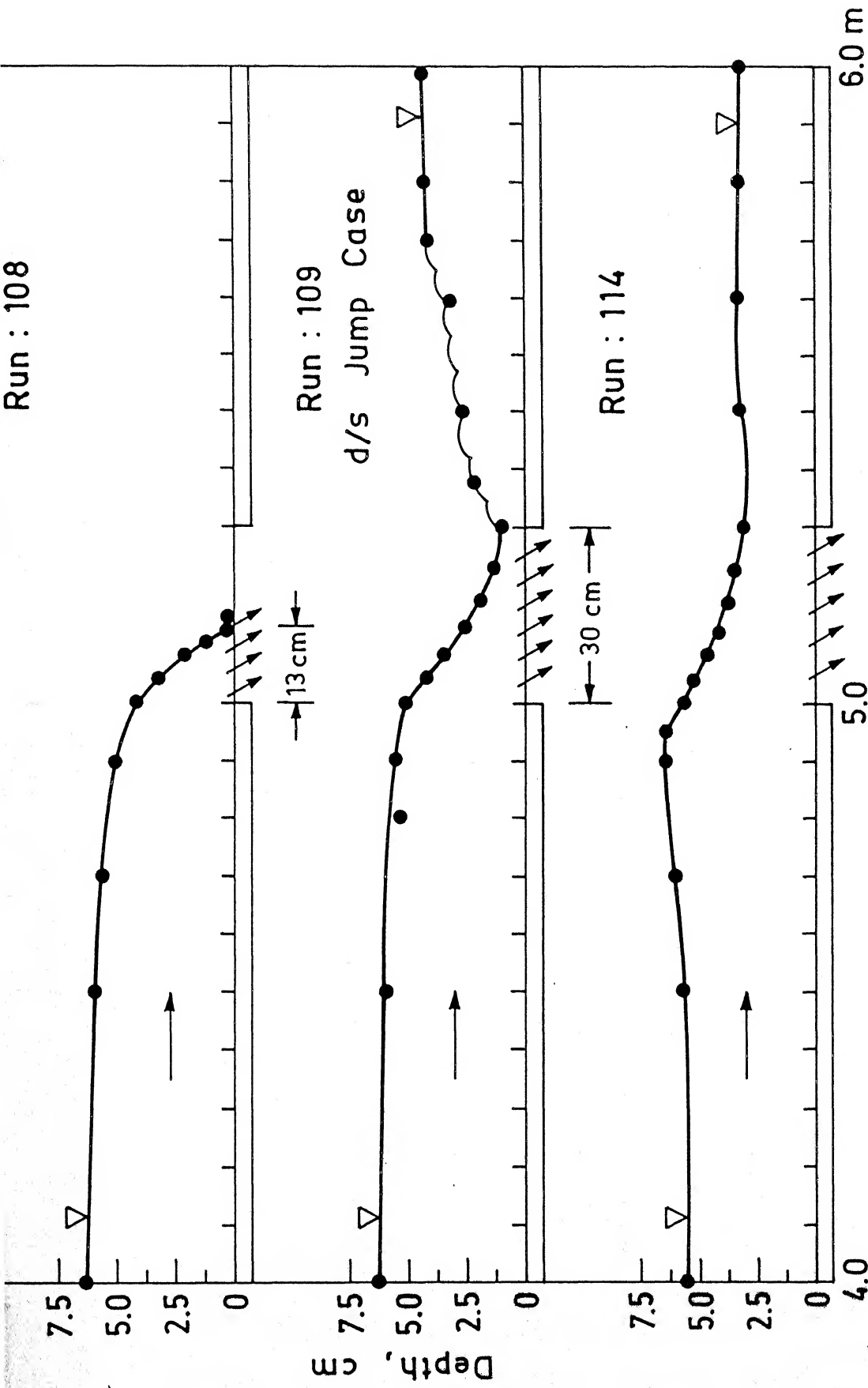


Fig. 3.5. Typical Water Surface Profiles for Super-critical Approach Flows (B1 Type).

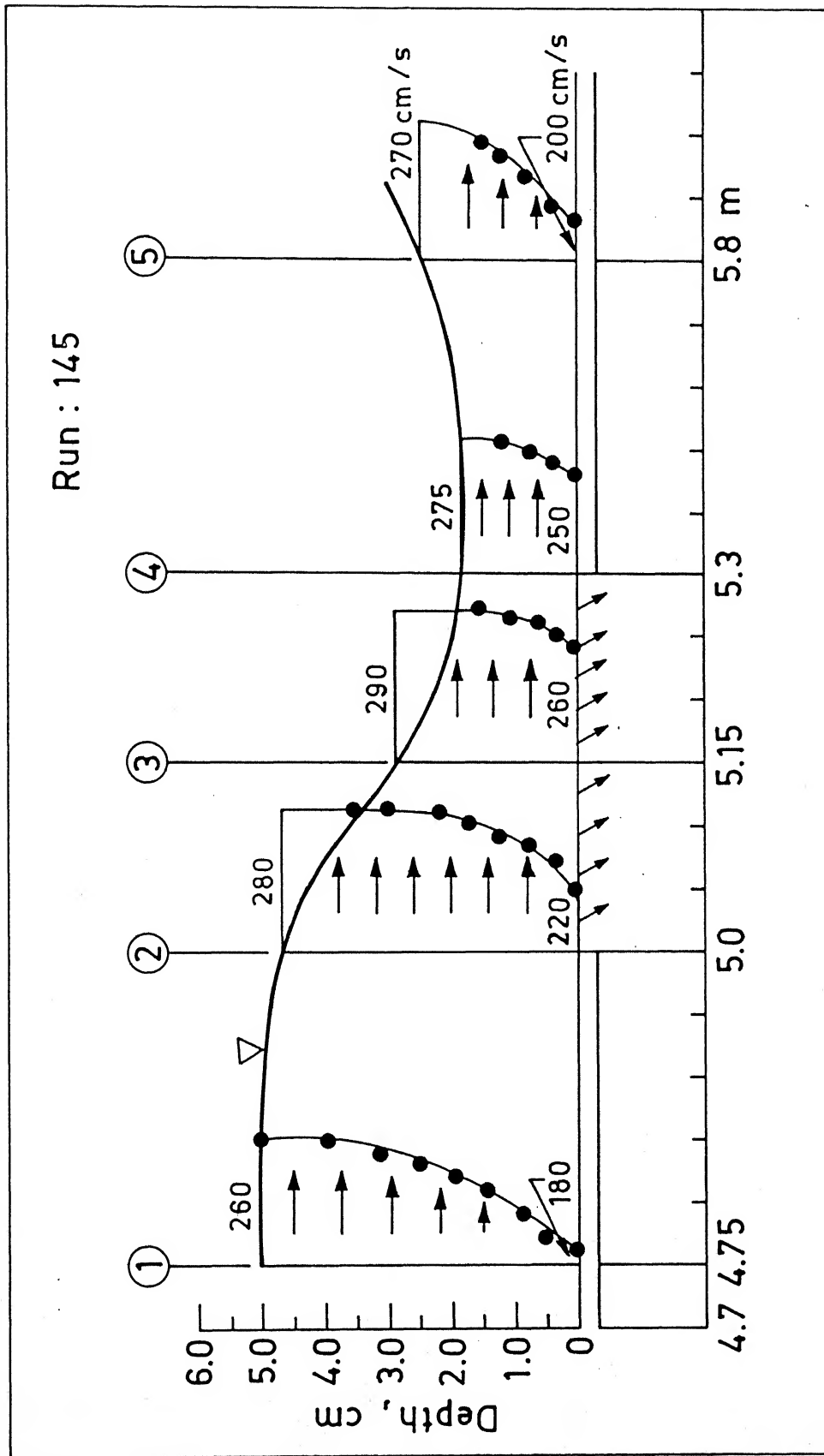


Fig. 3.6. Observed Typical Velocity Profiles.

CHAPTER IV

ANALYSIS

4.1 Study of The Limiting Inlet Depth:

4.1.1 Subcritical Approach Flows:

As indicated earlier in section 3.3.1 and shown in Fig. 3.3, three types of flows (viz, A1, A2, A3) are possible for subcritical approach flow case. The limiting inlet depth y_{1L} is introduced with a view to differentiate the free and submerged flows. For A1 and A2 types of flows the inlet depth $y_{1e} = y_{1L}$ and for A3 type of flow the inlet depth $y_{1e} > y_{1L}$. In a subcritical flow with a sudden drop, the depth y_{1L} will be the end depth. For rectangular channels, subcritical flows its value will be a constant at $0.715 y_c$. Also for any channel shape, in subcritical flows, the end depth ratio y_{1L}/y_c is independent of the Froude number (10). Hence, for A1 type flows over longitudinal bar bottom-racks, the ratio y_{1L}/y_c can be represented as

$$\frac{y_{1L}}{y_c} = \text{fn } (B/L, \epsilon) \quad (4.1)$$

Fig. 4.1 shows the variation of the limiting inlet depth ratio $\frac{y_{1L}}{y_c}$ with ϵ for $B/L = 2.0$ and 4.0 . It is seen that

$\frac{y_{1L}}{y_c}$ decreases with ϵ and is unaffected by the value of B/L . A best fit equation for the variation of the limiting

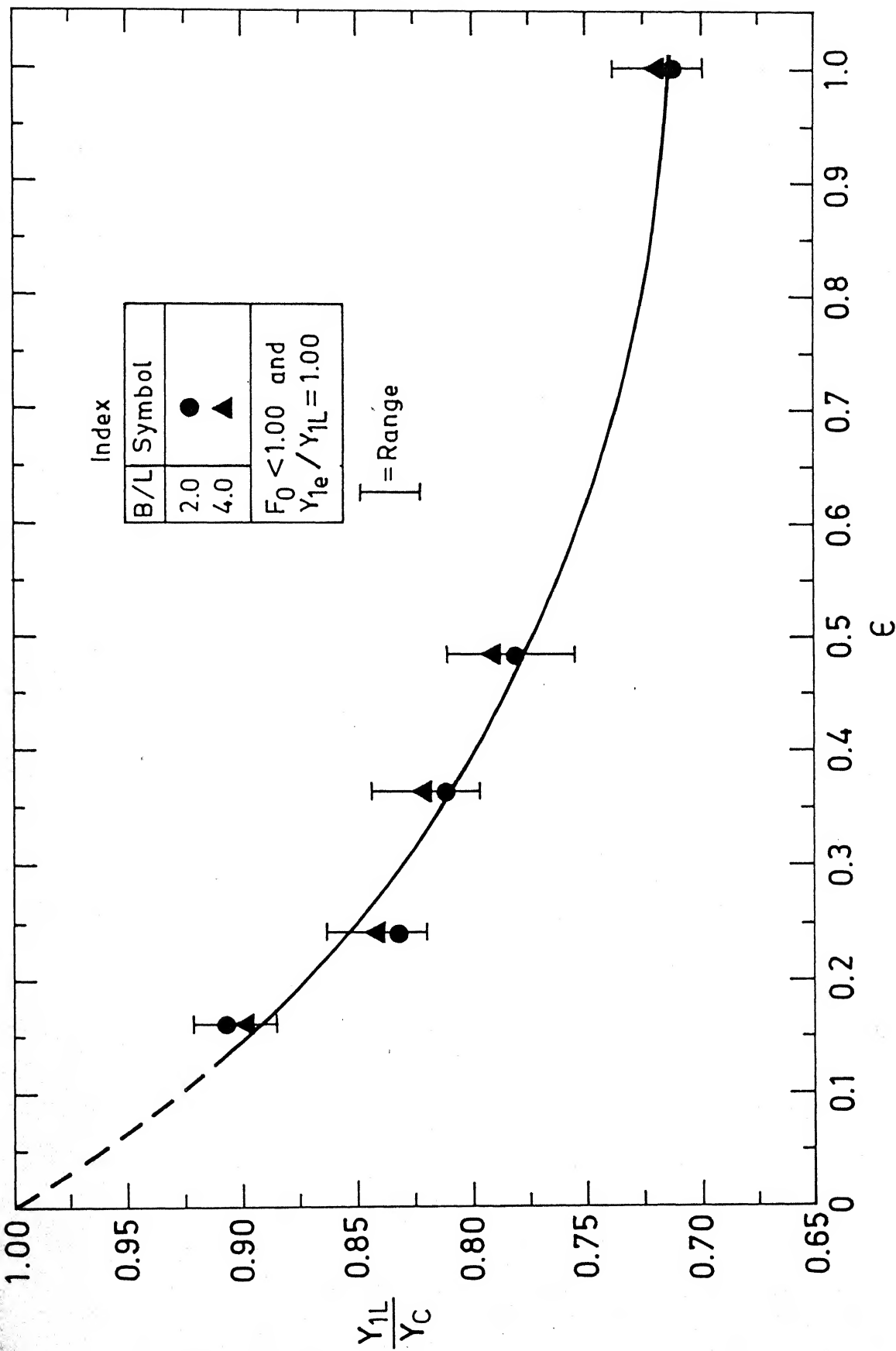


Fig. 4.1. Variation of Limiting Inlet Depth Ratio in Subcritical Approach Flows (A1 Type).

inlet depth ratio was obtained as

$$\frac{y_{1L}}{y_c} = -0.215 \log \epsilon + 0.715 \quad (4.2)$$

Eq.(4.2) is useful in determining the existence of A3 type flows.

4.1.2 Supercritical Approach Flows:

As indicated in section 3.3.2, in supercritical approach flows two types of flows over the rack are possible and these viz B1 and B2 type flows, are shown in Fig.3.3. From an analogy of end depths at sudden drops in supercritical flows, for B1 and B2 types of flows over racks $\frac{y_{1L}}{y_c}$ can be expected to be a function of Froude number also and can be represented as

$$\frac{y_{1L}}{y_c} = \text{fn} (B/L, \epsilon, F_o) \quad (4.3)$$

Fig. 4.3 shows the variation of $\frac{y_{1L}}{y_c}$ with ϵ and B/L , by taking F_o as a third parameter. It is seen that the B/L does not have any effect on $\frac{y_{1L}}{y_c}$. The effect of F_o on $\frac{y_{1L}}{y_c}$ for a given ϵ was found to be related by a linear relationship and the relation between the three parameters found by the best fit technique is:

$$\frac{y_{1L}}{y_c} = 0.915 - 0.137 F_o - 0.166 \epsilon \quad (4.4)$$

Fig. 4.4 shows the validity of Eq. (4.4). The correlation is very good and as such this Equation can be used with

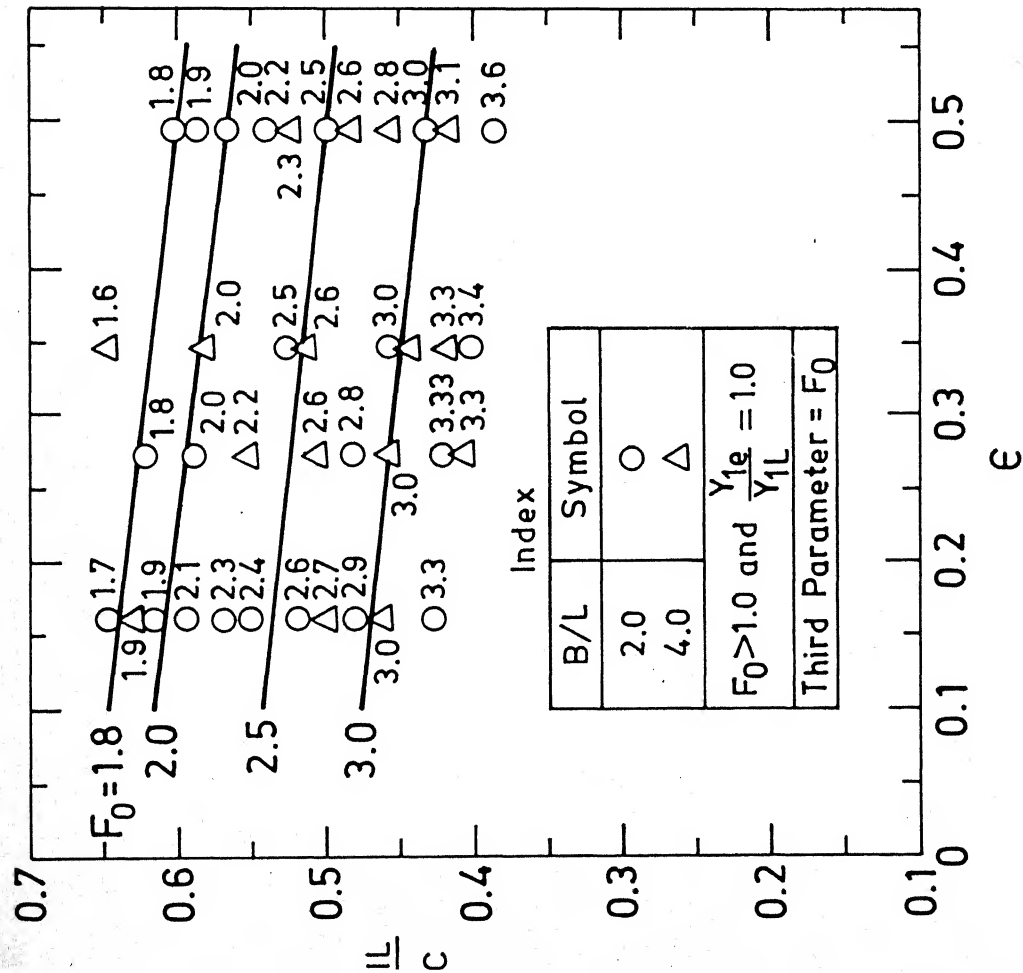


Fig. 4.2. Variation of Limiting Inlet Depth Ratio with ϵ and F_0 in Super-critical Approach Flows (B1 Type).

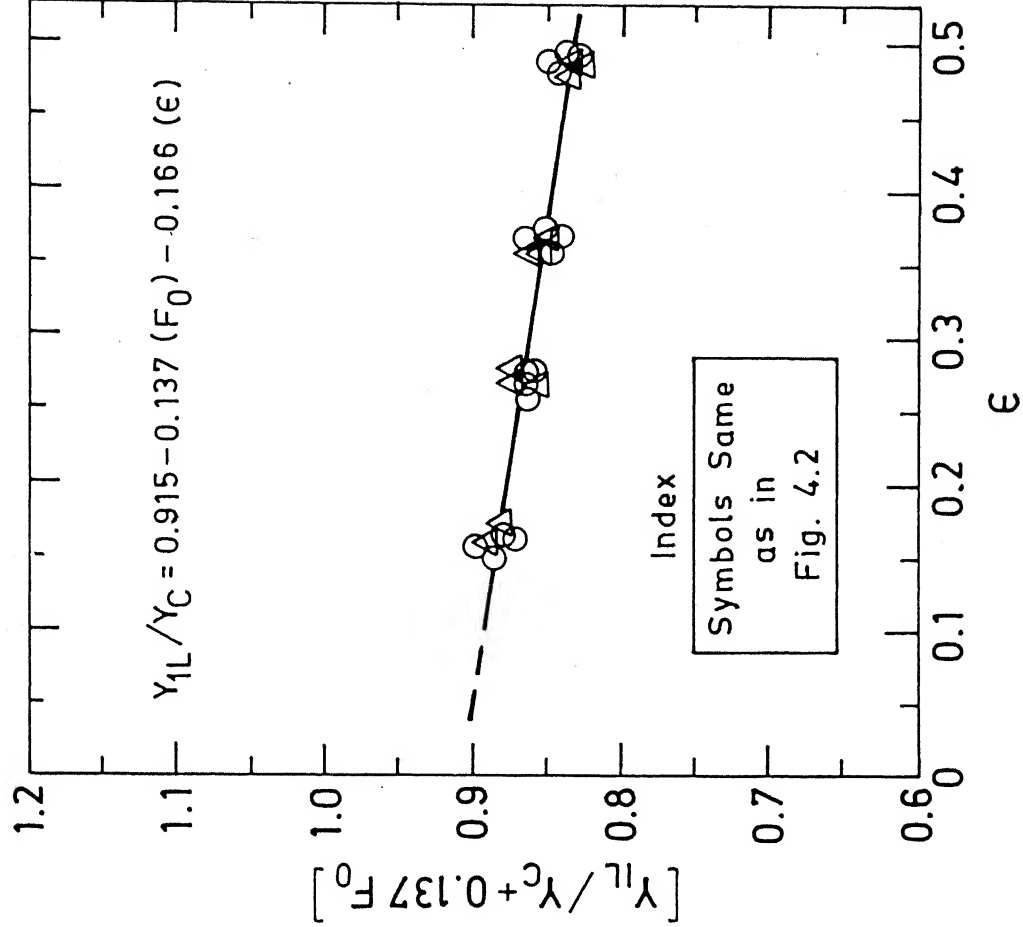


Fig. 4.3. Variation of Limiting Inlet Depth in Super-critical Approach Flows (B1 Type).

confidence for predicting y_{1L} in supercritical approach flows over longitudinal bar bottom-racks.

4.2 Study of The Coefficient of Discharge C_d :

4.2.1 Parameters:

The pressure distribution at the inlet of the rack will in general be different from the hydrostatic pressure distribution due to the curvature of the flow. In the extreme case of a sudden drop (and also a slot) it is known that the critical depth y_c occurs at about $5y_e$ and at that section the flow is essentially parallel and the hydrostatic pressure distribution exists there. As such a section at a distance of $5 y_{1e}$ upstream from the inlet was chosen for defining the approach flow parameters. At this section the specific energy E_o was taken as $E_o = y_o + \frac{V_o^2}{2g}$. Assuming an orifice type flow through the rack with an operating head equal to the energy head E_o over the entire rack, a coefficient of discharge C_d through the longitudinal bar bottom-racks is defined as

$$C_d = \frac{Q_D}{BL \sqrt{2gE_o}} \quad (4.5)$$

where Q_D = diverted flow through rack. The possible variables influencing C_d may be grouped as:

$$C_d = \text{fn}(V_o, y_o, B, L, D, S, g, \gamma), \text{ longitudinal slope} \quad (4.6)$$

Hence the dimensionless groups of variables will be

$$C_d = \text{fn} \left(\frac{V_o}{\sqrt{gy_o}}, \frac{V_o y_o}{\nu}, \frac{B}{y_o}, \frac{B}{L}, \frac{D}{S}, \frac{D}{B}, \text{longitudinal slope} \right) \quad (4.7)$$

For horizontal bottom-racks, longitudinal slope = 0 and for two dimensional flow cases $\frac{B}{y_o}$ may be considered to be an insignificant parameter. Out of the two rack parameters D/S is considered to be significant and the other viz, D/B can be considered to be insignificant especially for very low values of D/B . For turbulent flows $\frac{V_o y_o}{\nu} = \text{Reynolds number}$ of the approach flow being very high may be considered to have negligible effect over C_d . Hence for analysis in the practical ranges, the functional variation of C_d is taken as

$$C_d = \text{fn} \left[F_o, \frac{D}{S}, \frac{B}{L} \right] \quad (4.8)$$

If V = mean flow velocity in the channel, the resultant velocity V_r is given by $V_r = \sqrt{V^2 + 2gE}$ as shown in Fig.A4.05. The velocity through the rack, when assumed as an orifice flow, is directly proportional to $\sqrt{2gE}$, where E is the specific energy at any section over the rack. Also the parameter $\frac{V^2}{2gE} = \tan^2 \theta$ where θ = angle of inclination of the resultant velocity V_r with the vertical. Hence greater the angle θ lesser will be the effective area carrying the diverted flow. Hence lesser will be C_d . Thus $\frac{V^2}{2gE}$ seem to be an important parameter affecting the C_d . This parameter can be represented as

$$\frac{V^2}{2gE} = \frac{V^2}{(2gy + V^2)} = \frac{1}{(1 + 2/F^2)} \quad (4.9)$$

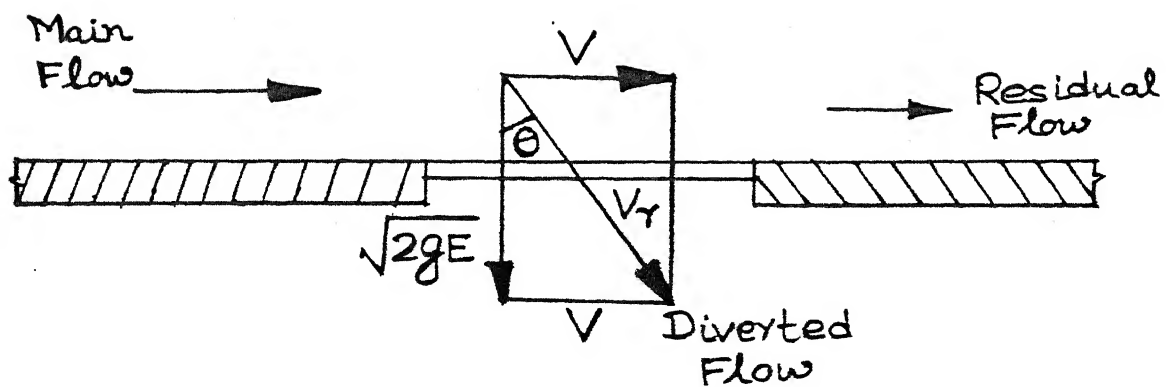


Fig. A 4.05

Velocity Triangle of the Flow
Diverting Through the Rack.

where F = Froude number of the flow at any section. For the purpose of analysis, the dimensionless parameter $\frac{v_o^2}{2gE_o}$ can be taken to be representative of $\frac{v^2}{2gE}$ for given rack and inlet conditions. In view of this, the parameter $\frac{v_o^2}{2gE_o}$ is used in the place F_o in Eq (4.8) to represent C_d as

$$C_d = \text{fn} \left(\frac{v_o^2}{2gE_o}, \frac{D}{S}, \frac{B}{L} \right) \quad (4.10)$$

It may be mentioned that a parameter similar to $\frac{v_o^2}{2gE_o}$ has also been used previously by Venkataraman, et al (4) and Ramamurthy, et al (6) to represent the approach velocity effect over the discharge coefficient through bottom-intakes. The term $\frac{v_o^2}{2gE_o}$ can be called as the Flow parameter for the rack. The parameter D/S is a measure of transverse contraction of the flow for a given opening area ratio. The parameter B/L is a measure of the two dimensionality of flow over the rack representing the possible effects of side walls.

The variation of C_d with the parameters given in Eq.(4.10) is analysed separately for A1, A3 and B1 types of flow.

4.2.2 C_d in A1 Flows:

For A1 flows the variation of C_d with $\frac{v_o^2}{2gE_o}$ by taking D/S as the third parameter is shown in Fig. 4.4. Four values of D/S in each of the two sets $B/L = 2.0$ and 4.0 respectively are plotted in this Figure. Also plotted are the results of experiments of flow over a slot. It is seen

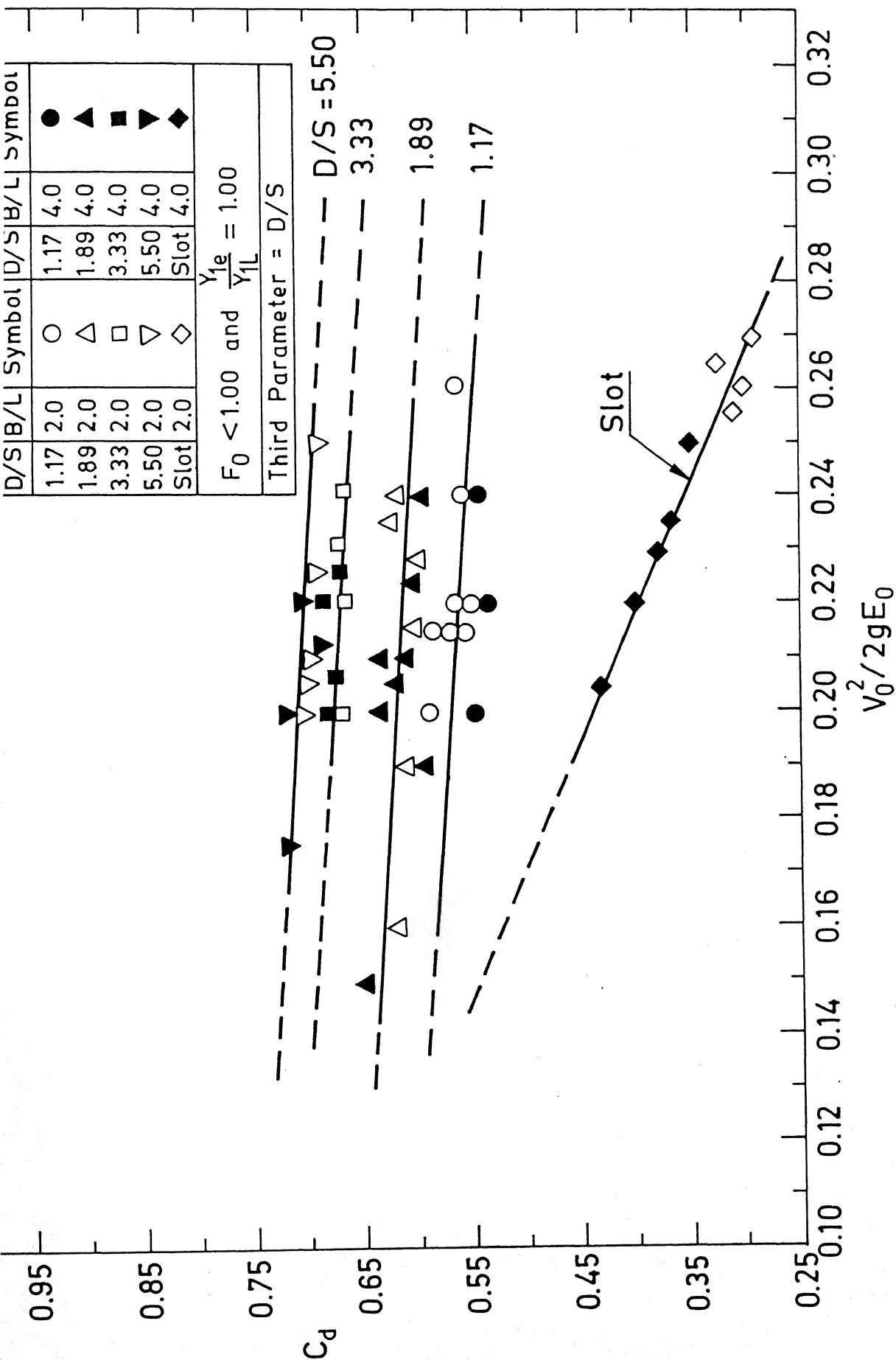


Fig. 4.4. Variation of C_d with $V_0^2/2gE_0$ and D/S in Subcritical Approach Flows (A1 Type).

that for a given D/S , there is no effect of B/L and the value of C_d decreases very slowly with $\frac{V_o^2}{2gE_o}$. The trend is consistent for all four values of D/S tested. The variation of C_d for a slot is appropriately located at low values of D/S . However, for a slot, the effect of $\frac{V_o^2}{2gE_o}$ is more pronounced, possibly due to the different nature of flow.

The variation of C_d for a given $\frac{V_o^2}{2gE_o}$ was found to be related by a logarithmic relation as

$$C_d = 0.2 \log (D/S) + 0.56 \quad (4.11)$$

within the range of D/S values tested (viz, $D/S = 1.17$ to 5.50). The best fit relation for the experimental data on Al flows was obtained as

$$C_d = 0.2 \log (D/S) - 0.247 \left(\frac{V_o^2}{2gE_o} \right) + 0.601 \quad (4.12)$$

This is shown in Fig. 4.5 where $[C_d - 0.2 \log (D/S)]$ is plotted against $\frac{V_o^2}{2gE_o}$ and all the data on Al flows are plotted, Eq. (4.12) is also shown in this Fig. It is interesting to observe the small scatters of data and hence the good correlation. As such, Eq. (4.12) can be taken to adequately represent the variation of C_d in Al flows for longitudinal bar bottom-racks. It may be noted that $\frac{V_o^2}{2gE_o}$ has a very small effect on C_d in Al flows, as the term $\frac{V_o^2}{2gE_o}$ will be within a value of 0.33. Hence, the second term in Eq. (4.12) can be neglected within 5 percent error.

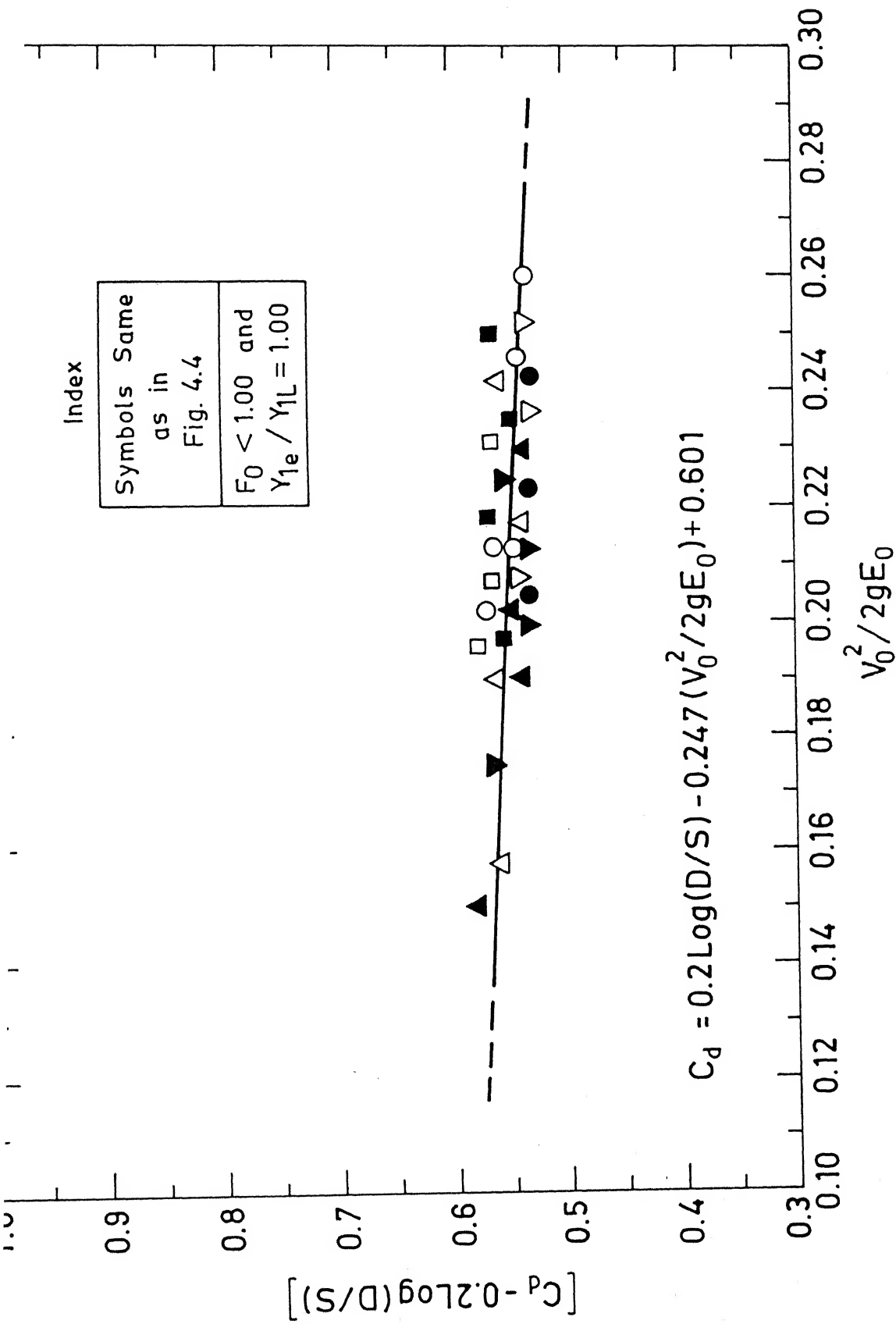


Fig. 4.5. Variation of C_d with D/S and $V_0^2 / 2gE_0$ in Subcritical Approach Flows (A1 Type).

4.2.3 C_d in A3 Flows:

For A3 flows C_d can be expected to be given by

$$C_d = \text{fn} \left[\frac{v_o^2}{2gE_o}, D/S, S_b \text{ and } B/L \right] \quad (4.13)$$

where S_b = submergence of the inlet = $\frac{y_{1e} - y_{1L}}{y_{1e}}$. For A3 flows the variation of C_d with $\frac{v_o^2}{2gE_o}$ by taking D/S as third parameter is shown in Fig. 4.6. Four values of D/S in each of the two sets $B/L = 2.0$ and 4.0 respectively are plotted in this figure, the data covers a range of submergence $S_b = 0.1$ to 0.55 . Also plotted are the results of experiments of flow over a slot. It is seen that for a given D/S , there is no effect of B/L and the value of C_d decreases with $\frac{v_o^2}{2gE_o}$. The trend is consistent for all four values of D/S tested. The variation of C_d for a slot is properly located at low values of D/S . Also there was no trend of variation of C_d with S_b . The variation of C_d for a constant $\frac{v_o^2}{2gE_o}$ was found to be related by a logarithmic relation as

$$C_d = 0.28 \log (D/S) + 0.57 \quad (4.14)$$

within the range of D/S values tested (viz, $D/S = 1.17$ to 5.50). The best fit relation for the experimental data on A3 flows was obtained as

$$C_d = 0.28 \log (D/S) - 0.565 \left(\frac{v_o^2}{2gE_o} \right) + 0.752 \quad (4.15)$$

This is shown in Fig. 4.7 where $[C_d - 0.28 \log (D/S)]$ is plotted against $\frac{v_o^2}{2gE_o}$ and all the data on A3 flows are plotted.

Eq.(4.15) is also shown. The maximum scatter of experimental

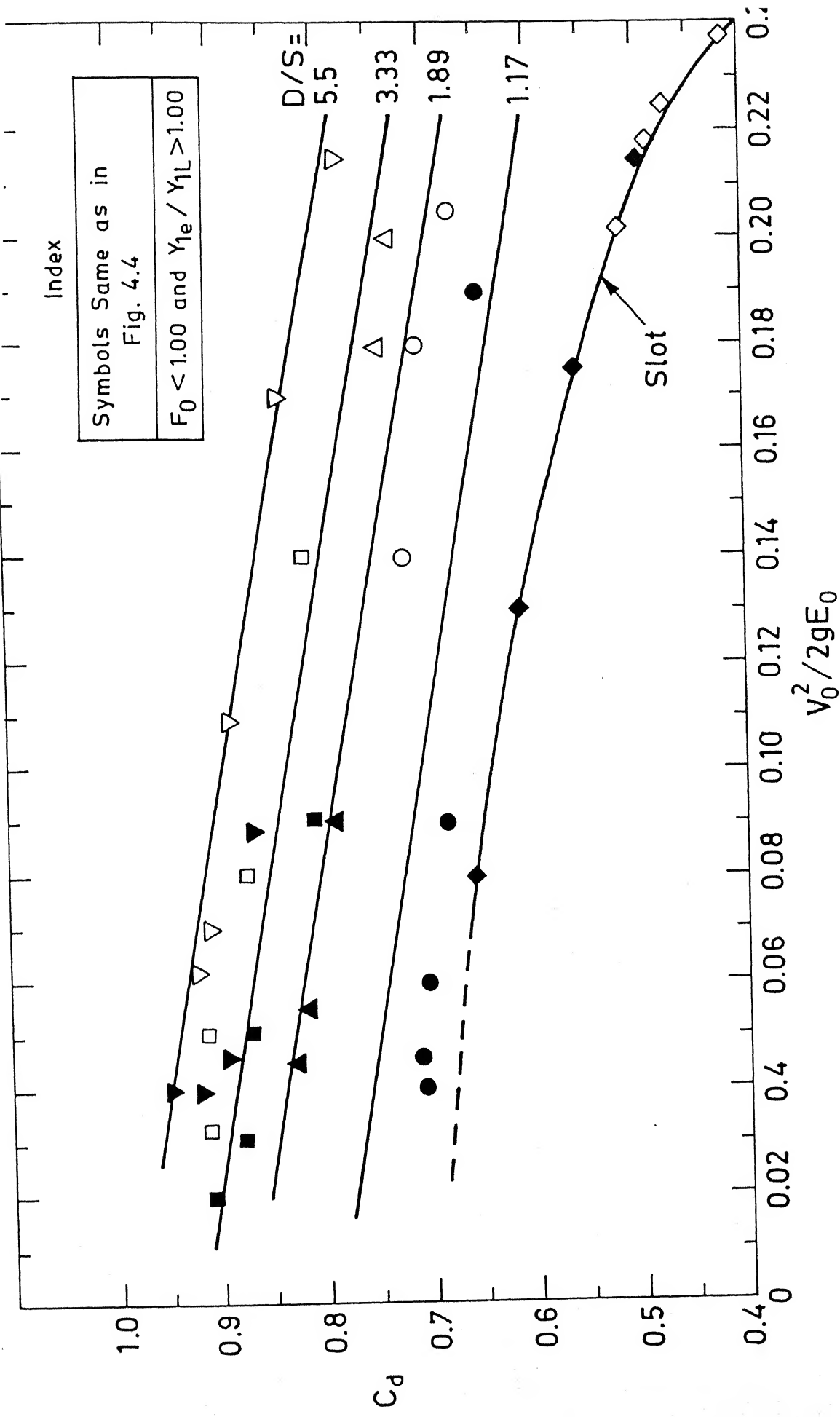


Fig. 4.6. Relation of C_d with $V_0^2 / 2gE_0$ and D/S in Subcritical Approach Flows (A3 Type).

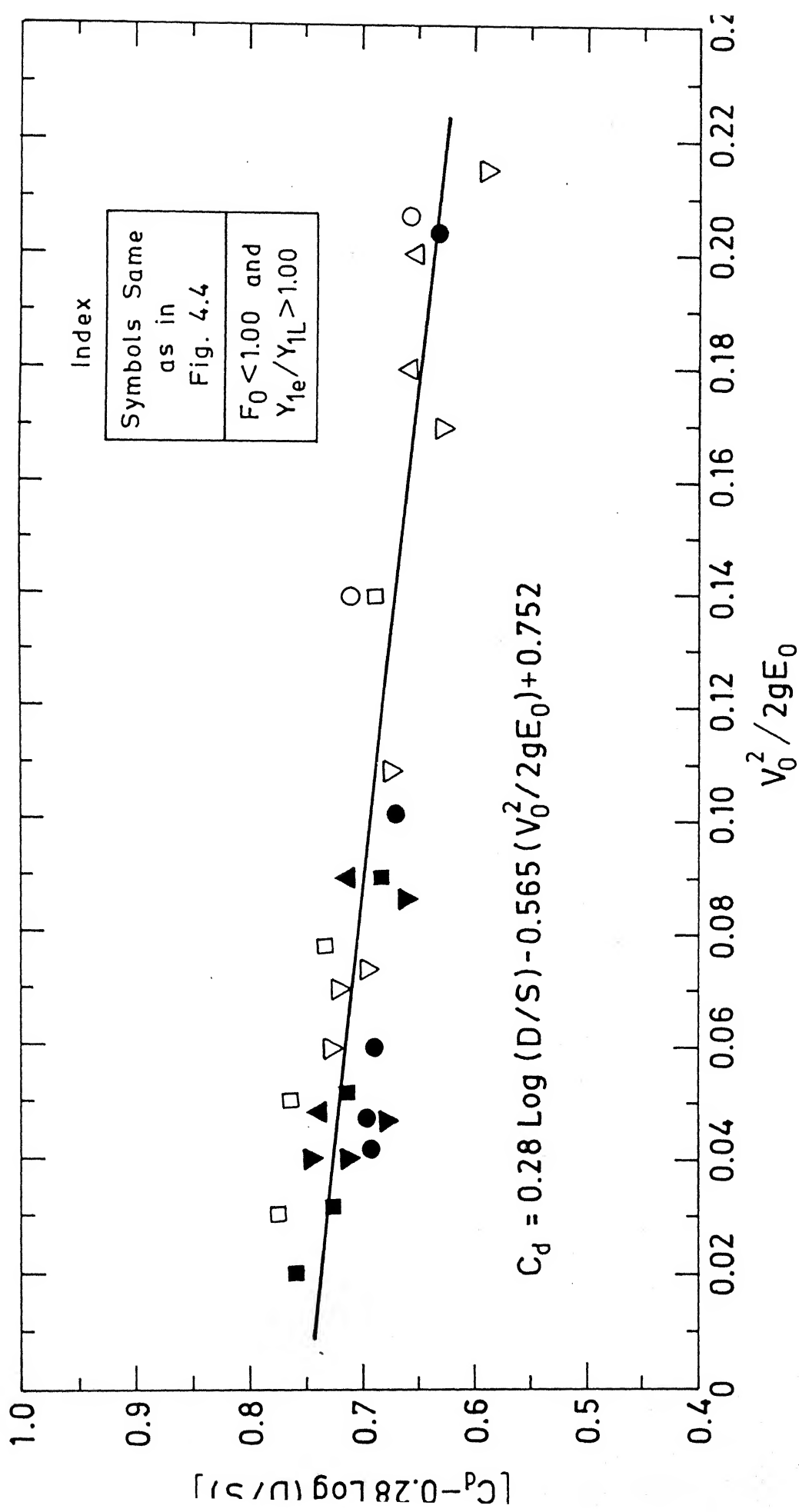


Fig. 4.7. Variation of C_d in Submerged Approach Flows (A3 Type).

data was found to be $\pm 6\%$. Hence, being a satisfactory correlation Eq. (4.15) can be taken to adequately represent the variation of C_d in A3 flows over longitudinal bar bottom-racks for submergence factor $S_b \leq 0.55$. It may be noted that, compared to A1 flows the values of C_d are higher in A3 flows. It is possible that at C_d is a weak function of S_b and at higher submergences Eq.(4.15) may have different coefficients.

4.2.4 C_d in B1 flows:

For B1 flows the variation of C_d with $\frac{V_o^2}{2gE_o}$ by taking D/S as third parameter is shown in Fig. 4.8. Four values of D/S in each of the two sets $B/L = 2.0$ and 4.0 respectively are plotted in this figure. It is seen that for a given D/S , there is no effect of B/L and the value of C_d decreases with $\frac{V_o^2}{2gE_o}$. The trend is consistent for all the four values of D/S tested. The variation of C_d for a constant $\frac{V_o^2}{2gE_o}$ was found to be related by a logarithmic relation as

$$C_d = 0.36 \text{ Log } (D/S) + 0.29 \quad (4.16)$$

within the range of D/S values tested (viz, $D/S = 1.13$ to 5.60). The best fit relation for the experimental data on B1 flows was obtained as

$$C_d = 0.36 \text{ Log } (D/S) - 1.084 \left(\frac{V_o^2}{2gE_o} \right) + 1.115 \quad (4.17)$$

This is shown in Fig. 4.9 where $[C_d - 0.36 \text{ Log } (D/S)]$ is plotted against $\frac{V_o^2}{2gE_o}$ and all the data on B1 flows are plotted. Eq.(4.17) is also shown in this Fig. The maximum scatter

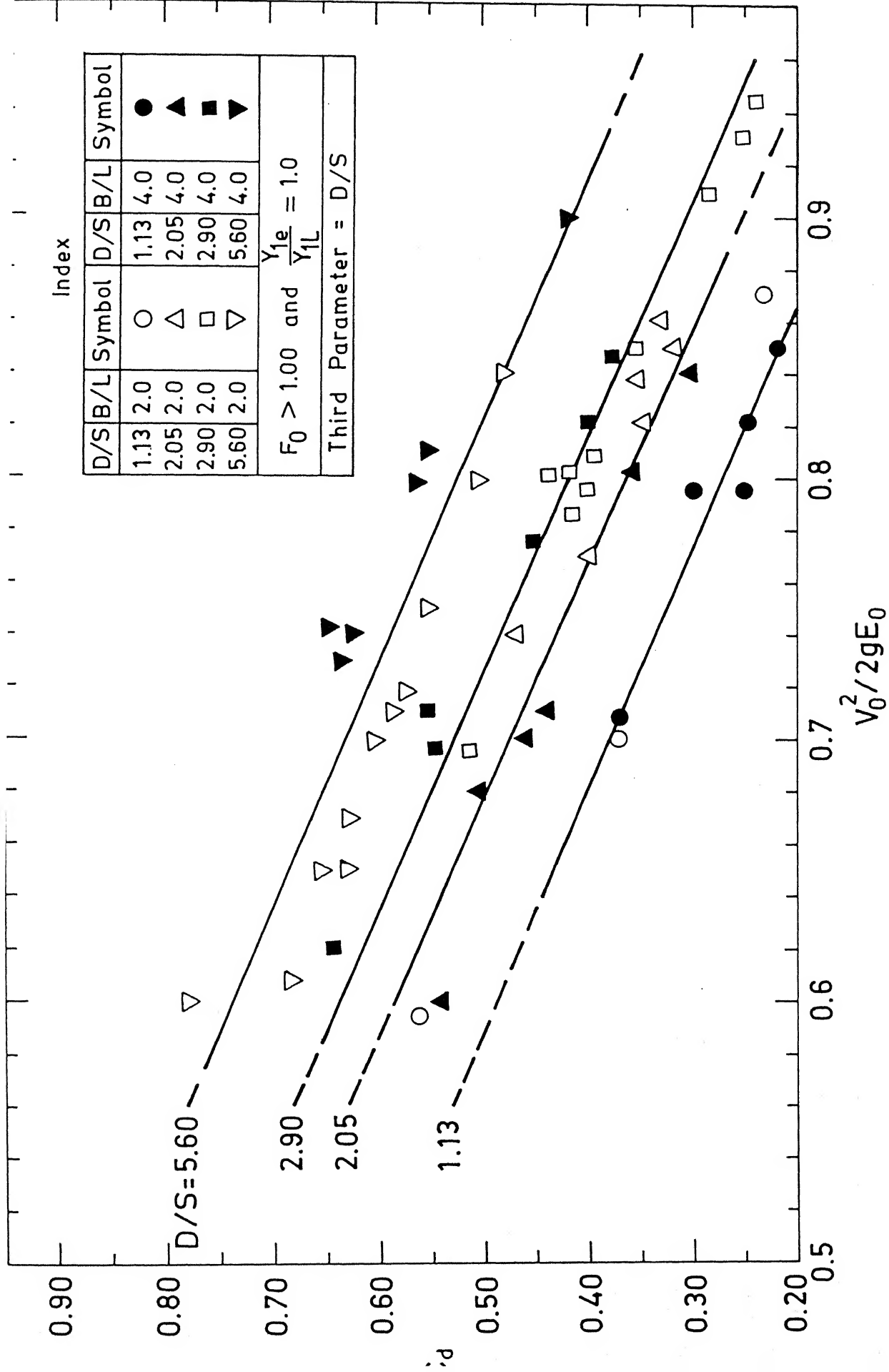
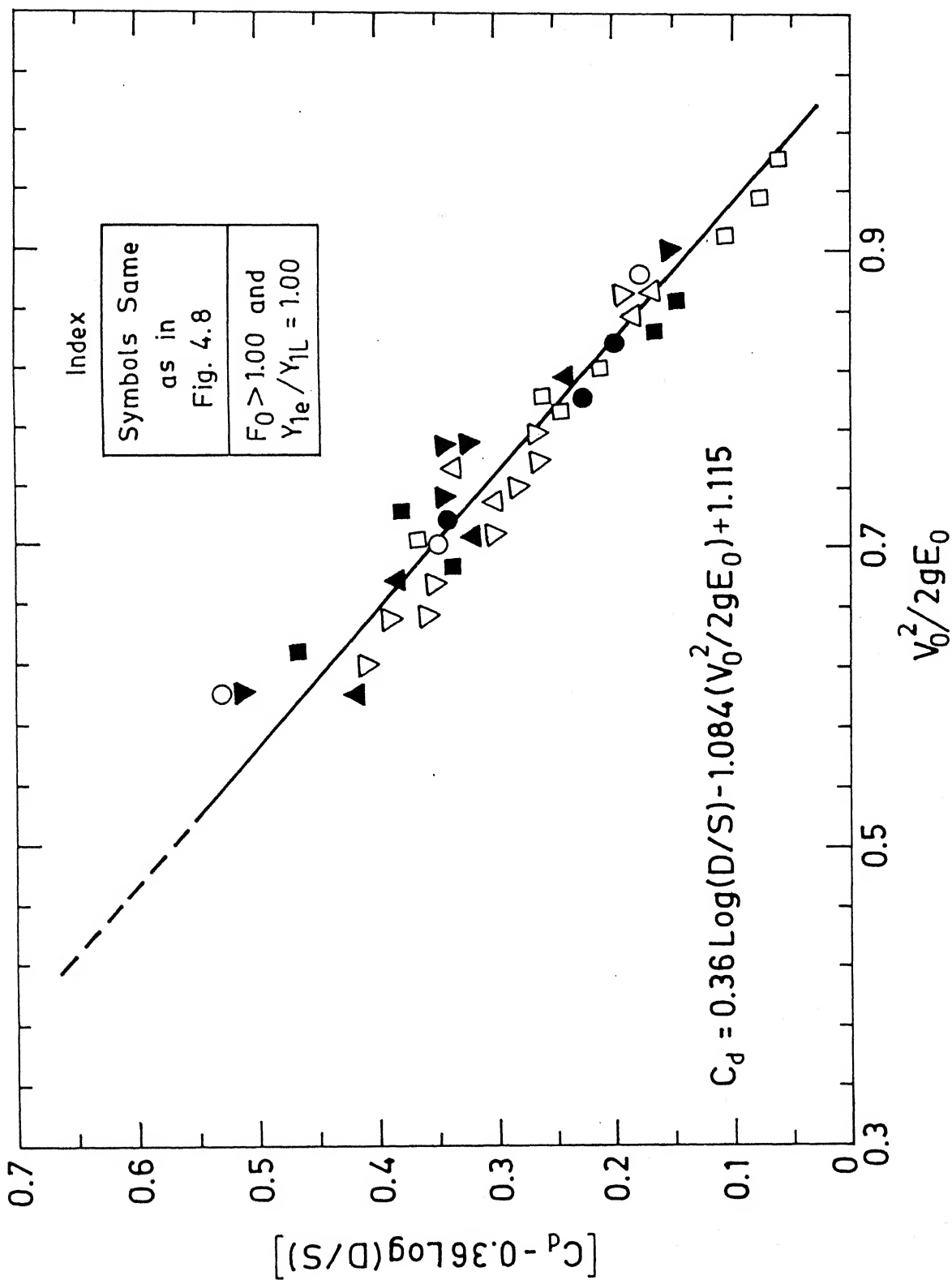


Fig. 4.8. Relation of C_d with $V_0^2/2gE_0$ and D/S in Super-critical Approach

Fig. 4.9 Variation of C_d in Super-critical Approach Flows

of experimental data was found to be $\pm 10\%$ with an average scatter of 3%, Hence, being a satisfactory correlation Eq. (4.17) can be taken to adequately represent the variation of C_d in Bl flows over longitudinal bar bottom-racks. It is noted that C_d values are affected considerably by the flow parameter $V_o^2/2gE_o$. For a given D/S ratio, C_d values rapidly decrease with increase in $V_o^2/2gE_o$ i.e. with the increase in Froude number of the approach flow.

4.3 Prediction of the Diversion Ratio:

4.3.1 Parameters

While the diverted flow Q_D for a given rack and flow condition can be calculated by using C_d , it is useful for design purposes to directly correlate the diversion ratio to the rack and flow parameters. The diversion ratio of a bottom-rack is defined as the ratio of flow diverted through the rack Q_D to the total stream flow Q_S i.e. Q_D/Q_S . The pertinent variables influencing the Q_D through a horizontal longitudinal bottom-rack may be grouped as

$$Q_D = \text{fn} [Q_S, y_o, \nu, g, B, L, D, S] \quad (4.18)$$

Hence, the dimensionless parameters affecting $\frac{Q_D}{Q_S}$ can be written as

$$\frac{Q_D}{Q_S} = \text{fn} \left[\frac{L^3 B^2 g}{Q_S^2}, \frac{Q_S}{B \nu}, \frac{D}{S}, \frac{D}{B}, \frac{B}{L}, \frac{B}{y_o} \right] \quad (4.19)$$

The dimensionless parameters in simplified form can be rewritten as

$$\frac{Q_D}{Q_S} = \text{fn} \left[\frac{L}{y_c}, R_{eo}, \frac{D}{S}, \frac{B}{L}, \frac{D}{B}, \frac{B}{y_o} \right] \quad (4.20)$$

where R_{eo} = Reynolds number of approach flow

y_c = upstream critical depth.

For turbulent flows, R_{eo} , being very high, may be considered to have negligible influence on the gross characteristics of the phenomenon. Out of the two rack parameters D/S is considered to be significant and the other viz, D/B is considered not significant at very small values. Further by assuming the effect of aspect ratio $\frac{B}{y_o}$ to be insignificant in 2D flows, the diversion ratio is expressed as

$$\frac{Q_D}{Q_S} = \text{fn} \left[\frac{L}{y_c}, \frac{D}{S}, \frac{B}{L} \right] \quad (4.21)$$

The parameter $\frac{L}{y_c}$ is a measure of the nature of approach flow and the size of the rack. It can be expected that the diversion ratio will increase with $\frac{L}{y_c}$. The parameter D/S is a measure of transverse contraction of the flow for a given opening area ratio. The parameter B/L is a measure of the two dimensionality of the flow over the rack representing the possible effects of side walls. It may be mentioned that the parameter $\frac{L}{y_c}$ has been used by Venkataraman, et al (4) for representing the variation of diversion ratio of a slot.

The variation of the diversion ratio with the parameters as in Eq. (4.21) is analysed separately for A1 and B1 flows.

4.3.2 $\frac{Q_D}{Q_S}$ in Al Flows

For Δ Al flows the variation of $\frac{Q_D}{Q_S}$ with $\frac{L}{y_c}$ by taking D/S as third parameter is shown in Fig. 4.10. Four values of D/S in each of the two sets $B/L = 2.0$ and 4.0 respectively are plotted in this figure. The value of $\frac{B}{y_o}$ in all the data was in the range 1.3-5.8. It can be observed that $\frac{Q_D}{Q_S}$ is not affected by B/L for a given D/S and increases linearly with $\frac{L}{y_c}$. Also, there is no specific effect of B/y_o . The trend is consistent for all the four D/S values tested. It is observed that the curve drawn through the experimental points passed through the origin in all the four cases of D/S . This is consistent with the boundary condition $Q_D = 0$ when $L = 0$ i.e., when there is no opening, there is no flow diversion. For a constant D/S , the diversion ratio can be expressed as

$$\frac{Q_D}{Q_S} = m_1 (L/y_c) \quad (4.23)$$

The slope m_1 is a function of D/S as seen in Fig. 4.10. The variation of m_1^* with D/S for Al flows is shown in Fig. 4.12, from which m_1 can be expressed as

$$m_1 = 0.51 - 0.41 \log (D/S) \quad (4.24)$$

Combining Eqs. (4.23) and (4.24)

$$\frac{Q_D}{Q_S} = [0.51 - 0.41 \log (D/S)] \frac{L}{y_c} \quad (4.25)$$

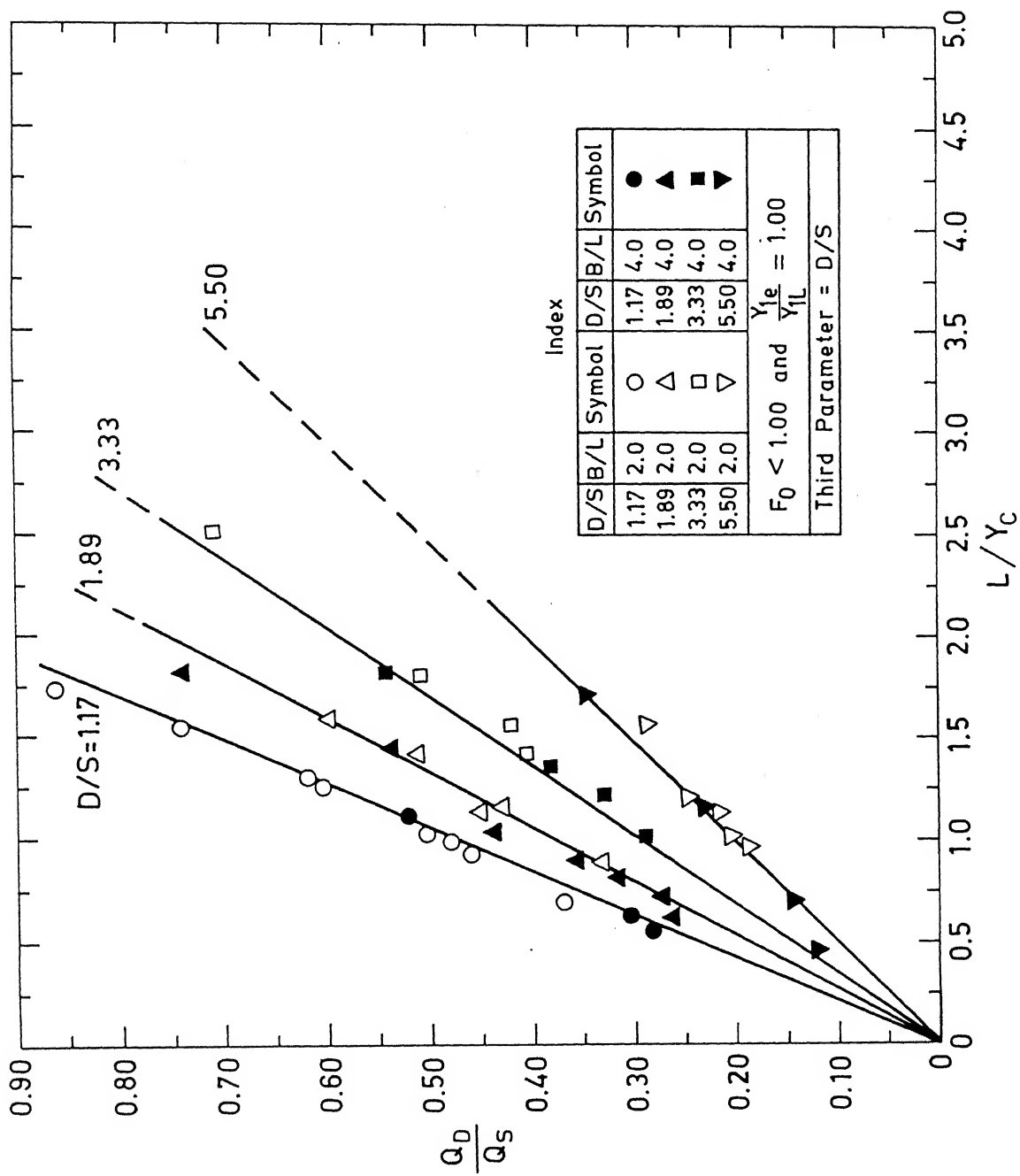


Fig. 4.10. Variation of Diversion Ratio in Subcritical Approach Flows (A1 Type).

The minimum length of rack to divert all the incoming flow, L_m is defined as the length causing 100% diversion. Hence, by putting $\frac{Q_D}{Q_S} = 1.0$ in Eq. (4.25)

$$L_{m1} = \frac{y_c}{[0.51 - 0.41 \log (D/S)]} \quad (4.26)$$

For a constant D/S , Eq. (4.25) is valid for $\frac{L}{y_c} \leq \frac{L_{m1}}{y_c}$ and for all $\frac{L}{y_c} > \frac{L_{m1}}{y_c}$ the $\frac{Q_D}{Q_S}$ will obviously be unity.

4.3.3 $\frac{Q_D}{Q_S}$ in Bl Flows

For Bl flows the variation of $\frac{Q_D}{Q_S}$ with $\frac{L}{y_c}$ by

taking D/S as third parameter is shown in Fig. 4.11. Four values of D/S in each of the two sets $B/L = 2.0$ and 4.0 respectively are plotted in this figure. The value of $\frac{B}{y_o}$ in all the data was in the range 6.98-15.38. It is seen that $\frac{B}{L}$ has no effect over $\frac{Q_D}{Q_S}$ for a given D/S while $\frac{Q_D}{Q_S}$ increases linearly with $\frac{L}{y_c}$. Also, $\frac{B}{y_o}$ has no distinct effect over the diversion ratio. The trend is consistent for all the four D/S values tested. Similar to A1 flows, in this case also the variation of Q_D/Q_S with L/y_c is linear and can be expressed by Eq. 4.25, replacing m_1 by m_2 .

The slope m_2 is a function of D/S as seen in Fig. 4.11. The variation of m_2^* with D/S for Bl flows is also shown in Fig. 4.12, from which m_2 can be expressed as

$$m_2 = 0.36 - 0.26 \log (D/S) \quad (4.27)$$

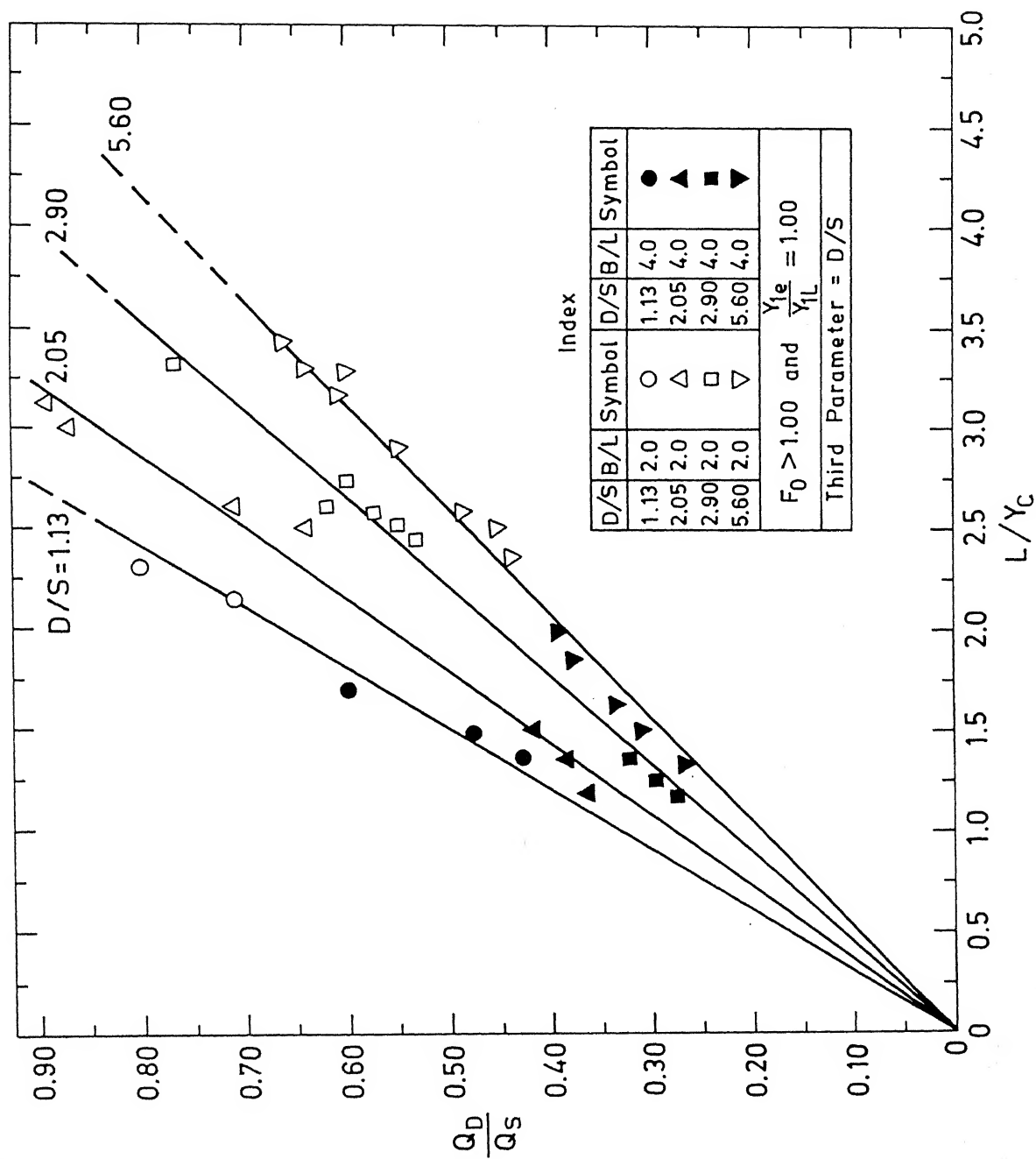


Fig. 4.11. Variation of Diversion Ratio in Super-critical Approach Flows (B1 Type).

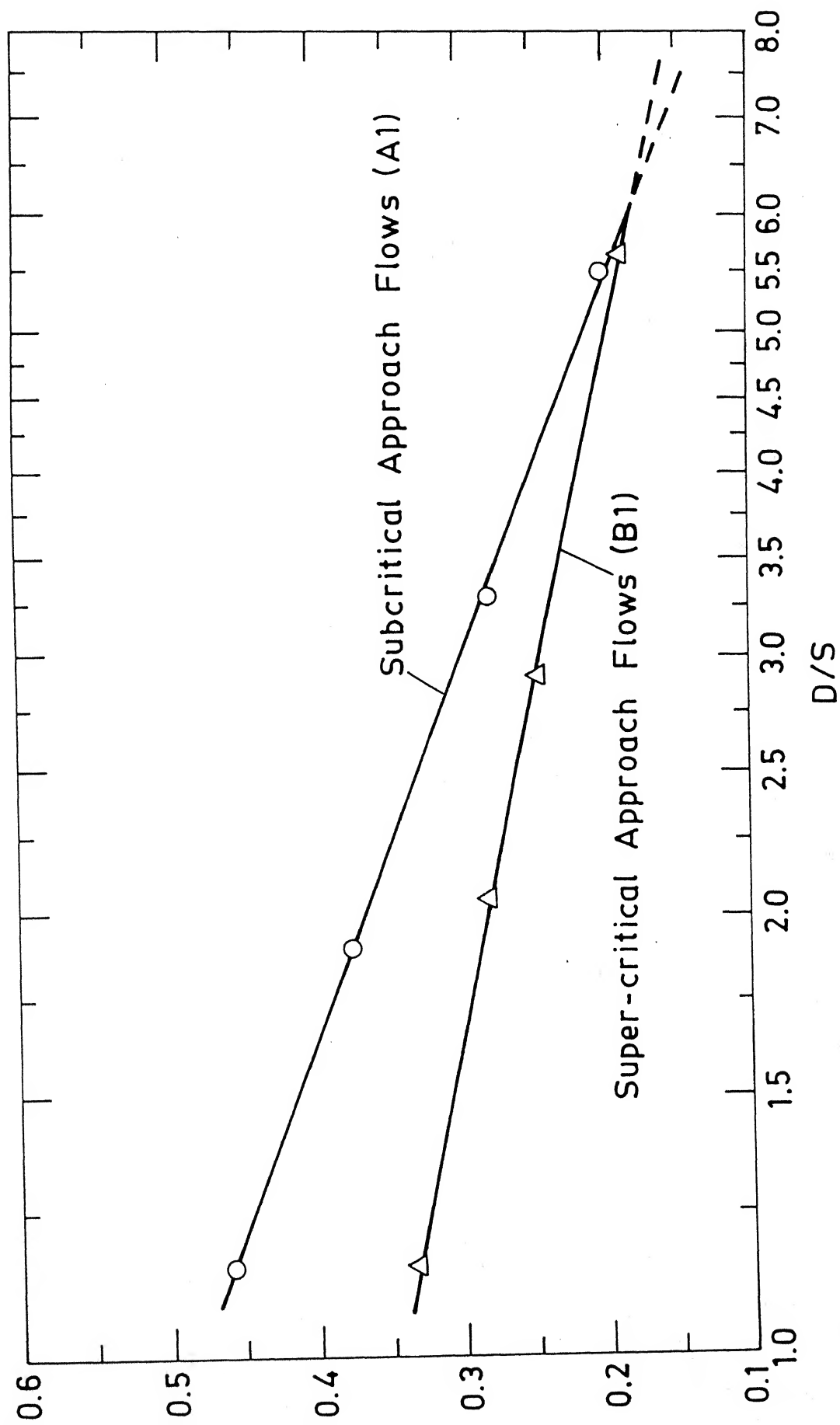


Fig. 4.12. Relation of m with D/S .

Combining Eqs.(4.23) and (4.27)

$$\frac{Q_D}{Q_S} = [0.36 - 0.26 \log (D/S)] \frac{L}{Y_c} \quad (4.28)$$

Further the minimum length L_{m_2} in Bl flows can be represented as

$$L_{m_2} = \frac{Y_c}{[0.36 - 0.26 \log (D/S)]} \quad (4.29)$$

As in Al flows, for a constant D/S , Eq.(4.28) is valid till $\frac{L}{Y_c} \leq \frac{L_{m_2}}{Y_c}$ and for all $\frac{L}{Y_c} > \frac{L_{m_2}}{Y_c}$, Q_D/Q_S will be unity.

It is observed that for a given $\frac{L}{Y_c}$ and D/S , the diversion ratio is higher in Al flows than in Bl flows.

* In Fig. 4.12, $m=m_1$ (for Al flows) and $m=m_2$ (for Bl flows).

4.3.4 $\frac{Q_D}{Q_S}$ in Al flows over a Slot:

For Al flows over a slot the variation of $\frac{Q_D}{Q_S}$ with

$\frac{L}{Y_c}$ is shown in Fig. 4.13. The experimental data of the present study for the two sets $B/L = 2.0$ and 4.0 along with the experimental data from Venkataraman (4) for $B/L = 2.0$ and 5.0 are plotted in this Figure. It is seen that $\frac{B}{L}$ does not affect the diversion ratio distinctly. Diversion ratio varies linearly with $\frac{L}{Y_c}$ and can be expressed as

$$\frac{Q_D}{Q_S} = 0.5883 \left(\frac{L}{Y_c} \right) \quad (4.30)$$

From this equation for Al flows over a slot, $\frac{L_m}{Y_c} = 1.7$. The Eq.(4.30) is valid for $\frac{L}{Y_c} \leq \frac{L_m}{Y_c}$ and for all values of

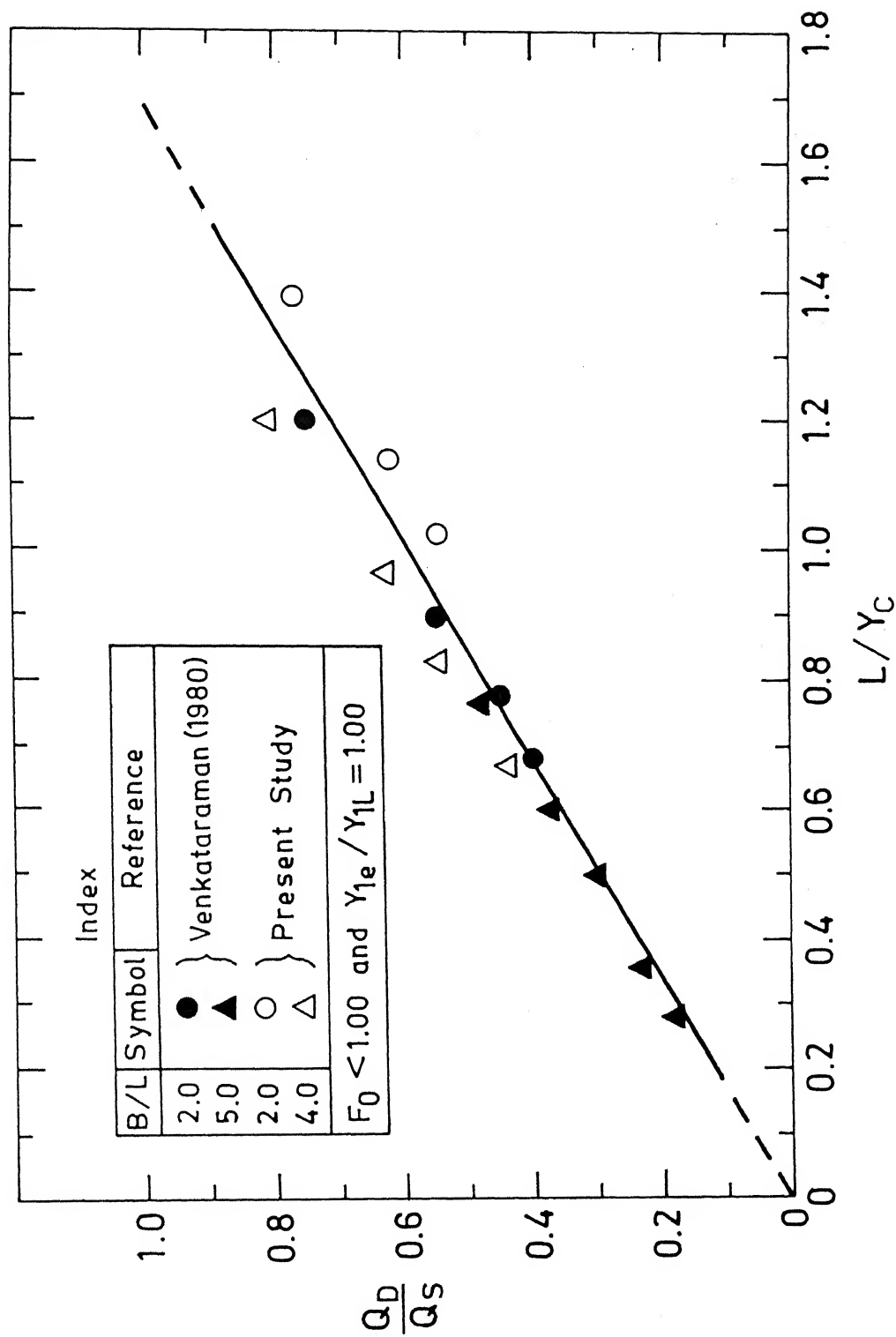


Fig. 4.13. Variation of Diversion Ratio for a Slot in Sub-critical Approach Flows (A1 Type).

$\frac{L}{y_c} > \frac{L_m}{y_c}$ the diversion ratio will be unity, where L_m = minimum length of the slot required for 100% diversion.

4.4 Energy Loss Over the Rack:

4.4.1 Introduction:

For determining the energy loss E_L over the rack, the specific energy at the inlet to the rack E_1 was defined as $E_1 = y_{1e} + \frac{v_1^2}{2g}$ by ignoring the correction for curvilinear flow over this section. Thus the energy loss over the horizontal rack can be approximated without serious error as

$$E_L = E_1 - E_2 = (y_{1e} + \frac{v_1^2}{2g}) - (y_{2e} + \frac{v_2^2}{2g}) \quad (4.31)$$

where suffix 2 represents the conditions at section 2. It is common in spatially varied flow analysis (for example Mostkow (3)) to assume the energy loss over the rack as negligibly small. As such, a study was made to find out the order of magnitude of the energy loss in the present investigation.

Plots of $\frac{E_L}{E_1}$ vs $\frac{L}{y_{1e}}$ for A1 and B1 flows are shown in Figs. 4.14 and 4.15 respectively. It is seen that in both these flows there is considerable energy loss even though there is no direct correlation with $\frac{L}{y_{1e}}$. The average value of $\frac{E_L}{E_1}$ in A1 flows is around 15% while it is about 30% in B1 flows. Also it was found that $\frac{E_L}{E_1}$ is not correlated with F_I in both A1 and B1 flows.

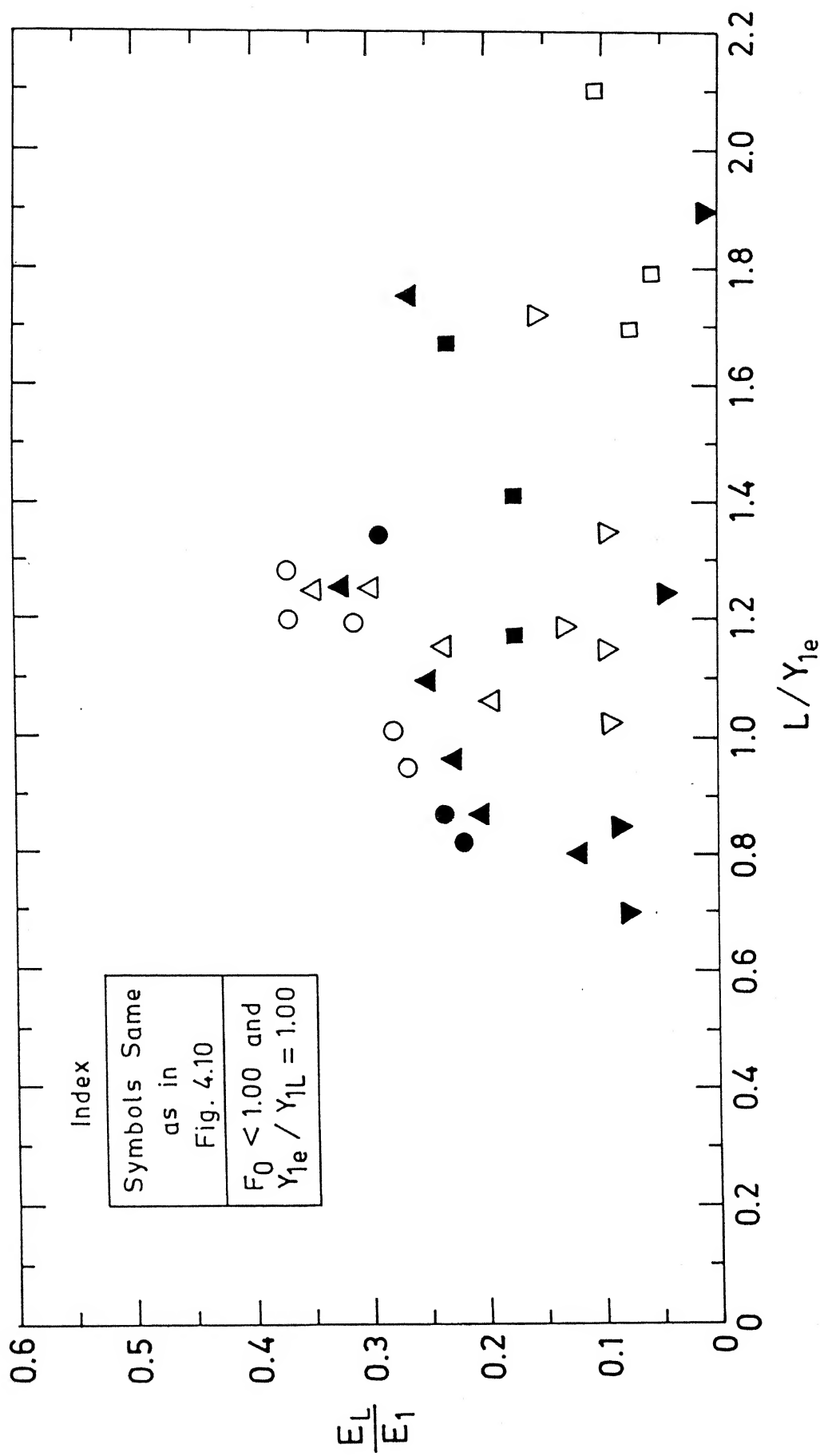


Fig. 4.14. Variation of Energy Loss Over the Rack in Subcritical Approach Flows (A1 Type).

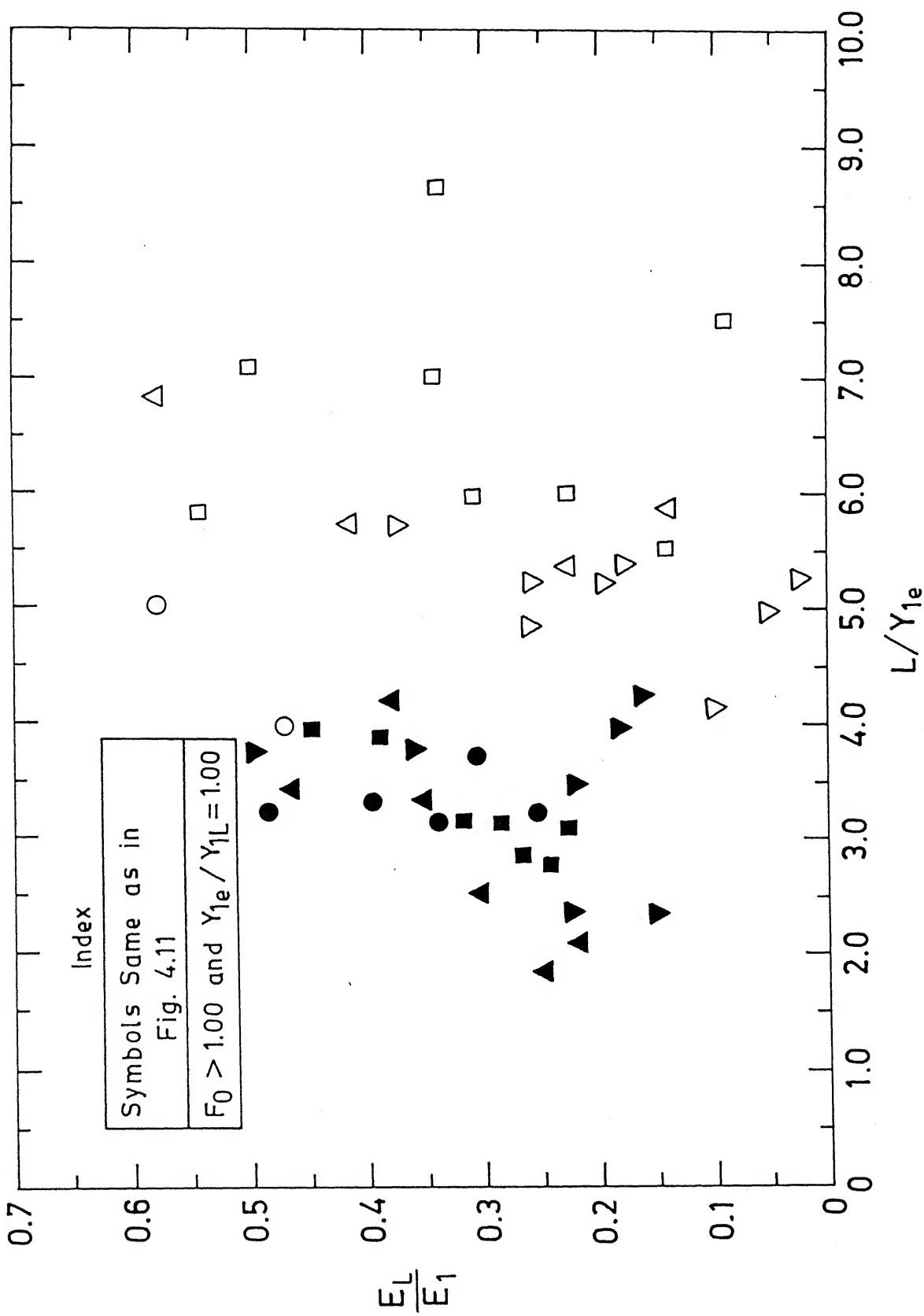


Fig. 4.15. Variation of Energy Loss Over the Rack in Supercritical Approach Flows (B1 Type).

In a simple model E_L was defined as

$$E_L = K \frac{V_1^2}{2g} \quad (4.32)$$

where K is the coefficient of energy loss. While an average value of K was obtained as 0.4 in both A1 and B1 flows, there was considerable scatter and no distinct correlation with either F_1 or L/y_{1e} could be obtained.

In another model the energy slope $S_e = E_L/L$ was expressed as

$$S_e = \text{fn} (B, L, y_{1e}, D, S) \quad (4.33)$$

Groups of dimensionless variables affecting the variation of S_e can be written as

$$S_e = \text{fn} \left(\frac{L}{y_{1e}}, \frac{D}{S}, \frac{B}{L} \right) \quad (4.34)$$

The variation of S_e with the parameters as in Eq. (4.34) is analysed separately for A1 and B1 flows.

4.4.2 S_e in A1 flows:

For A1 flows the variation of S_e with $\frac{L}{y_{1e}}$ by taking D/S as the third parameter is shown in Fig. 4.16. Four values of D/S in each of the two sets $B/L = 2.0$ and 4.0 respectively are plotted in this figure. It is seen that for a given D/S there is no effect of B/L and the value of S_e decreases with $\frac{L}{y_{1e}}$. The trend is consistent for all the four D/S values tested. The variation of S_e for a constant $\frac{L}{y_{1e}}$ was found to be related by a linear relation within the range of D/S values tested (viz, $D/S = 1.17$ to 5.50) as

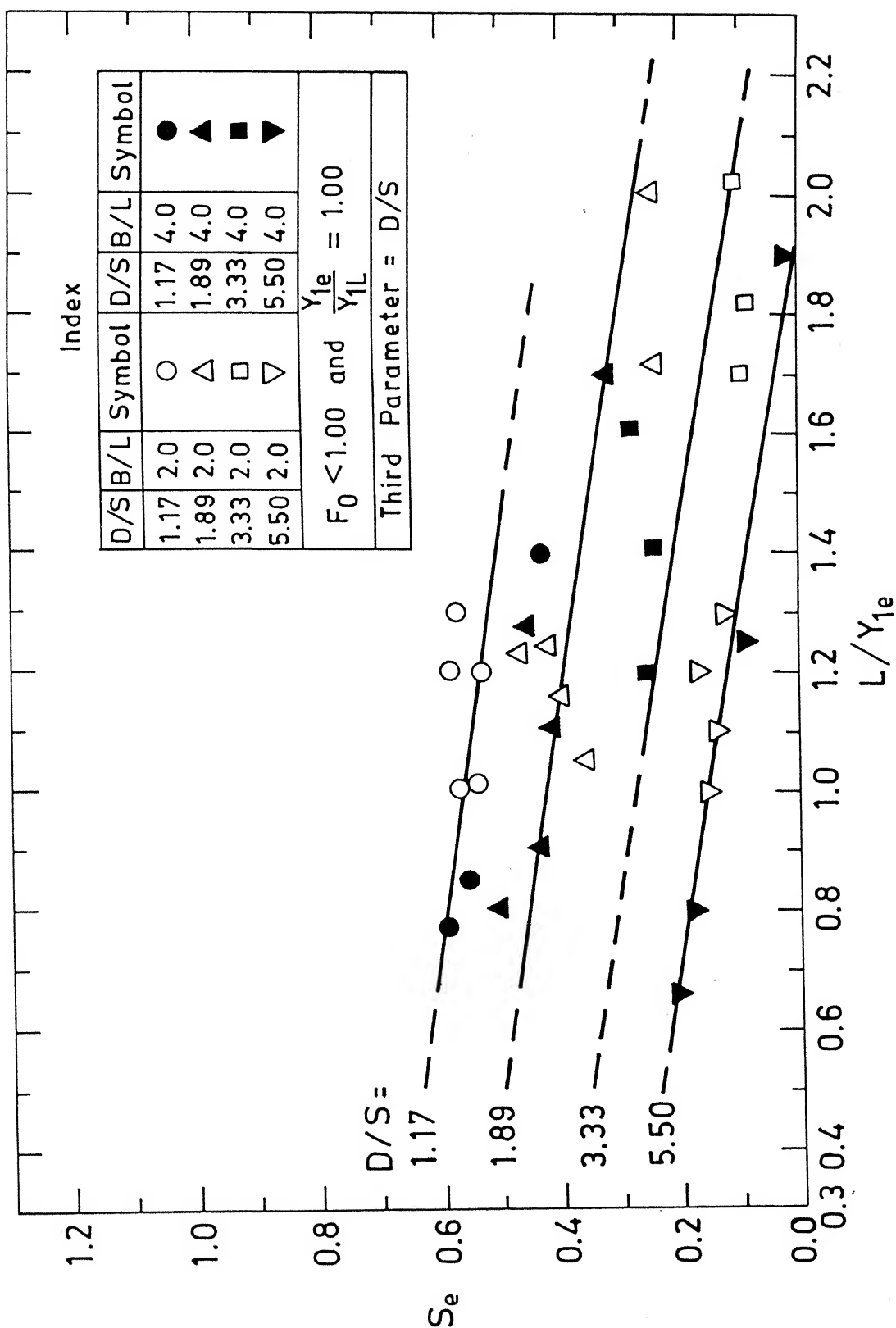


Fig. 4.16. Relation of Energy Slope with L/Y_{1e} and D/S in Subcritical Approach Flows (A1 Type).

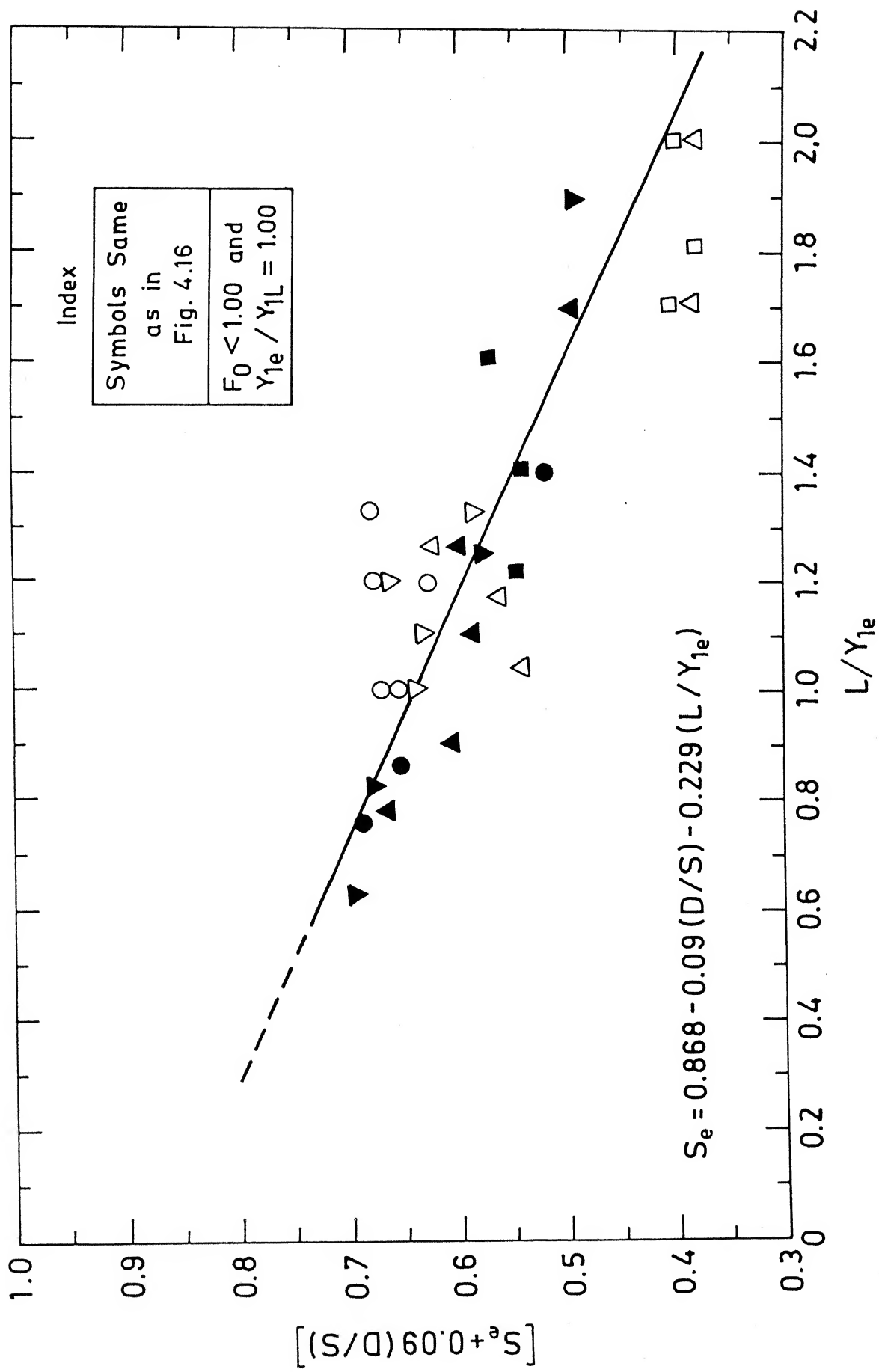


Fig. 4.17. Variation of Energy Slope Over the Rack in Subcritical Approach Flows (A1 Type).

$$S_e = 0.785 - 0.09 (D/S) \quad (4.35)$$

Using this the best fit relation for the experimental data on Al flows was obtained as

$$S_e = 0.868 - 0.09 (D/S) - 0.229 (L/y_{1e}) \quad (4.36)$$

This is shown in Fig. 4.17 where $[S_e + 0.09 (D/S)]$ is plotted against $\frac{L}{y_{1e}}$ and all the data on Al flows are plotted. Eq. (4.36) is also shown in this Fig. The maximum scatter of the data was found to be $\pm 15\%$ and the average scatter was about 5%. Hence, this equation can satisfactorily be used for the estimation of the energy slope in Al flows over longitudinal bar bottom- racks.

4.4.3 S_e in Bl flows:

For Bl flows the variation of S_e with $\frac{L}{y_{1e}}$ by taking D/S as the third parameter is shown in Fig. 4.18. Four values of D/S in each of the two sets $B/L=2.0$ and 4.0 respectively are plotted in this figure. It is noted that for a given D/S there is no effect of B/L and the value of S_e decreases with $\frac{L}{y_{1e}}$. The trend is consistent for all the four D/S values tested. The variation of S_e for a constant $\frac{L}{y_{1e}}$ was found to be related by a linear relation as

$$S_e = 1.01 - 0.09 (D/S) \quad (4.37)$$

within the range of D/S values tested (viz, $D/S = 1.13$ to 5.60). The best fit relation for the experimental data on Bl flows was obtained as

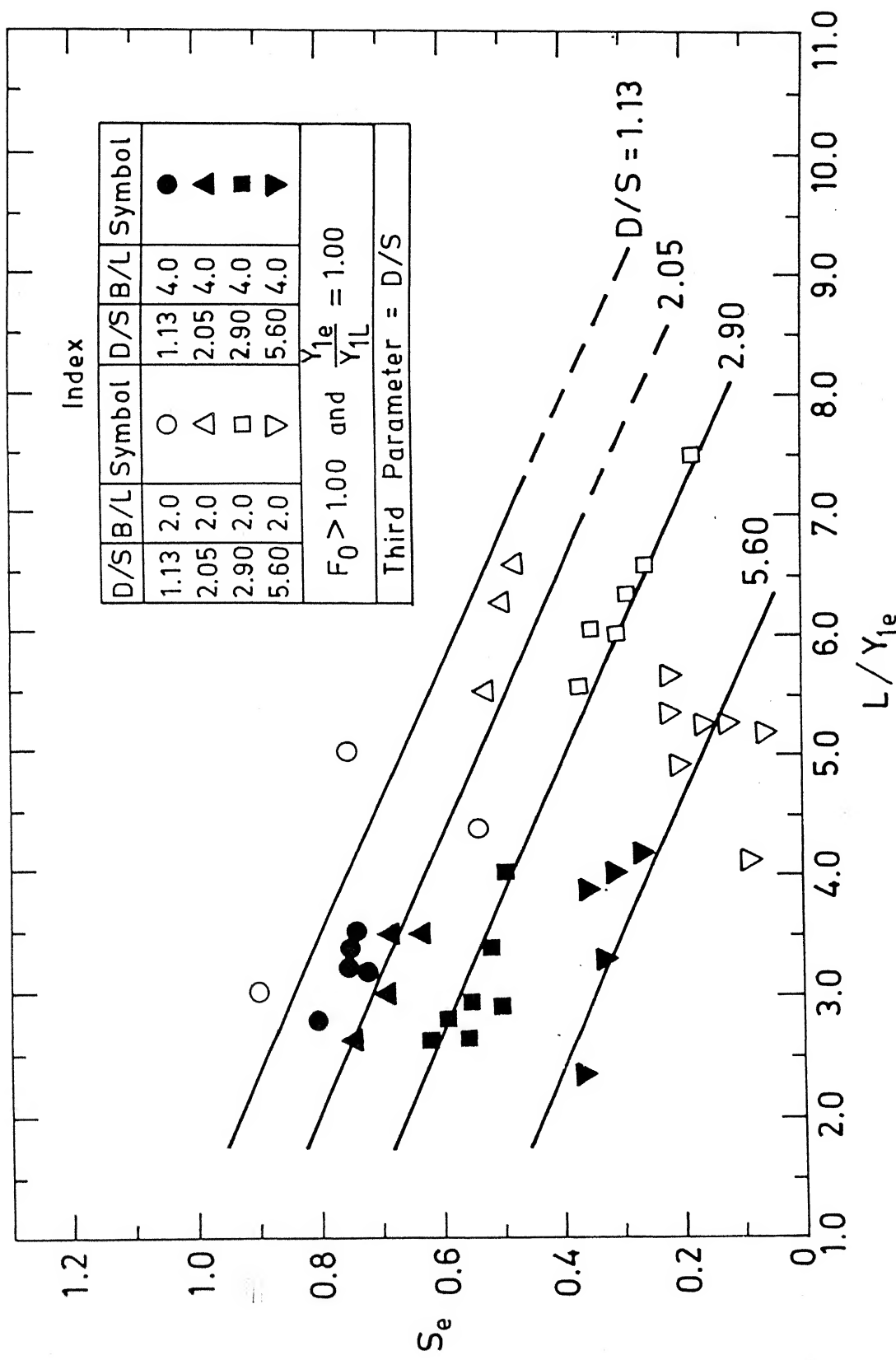


Fig. 4.18. Relation of Energy Slope with L/Y_{1e} and D/S in Super-critical Approach Flows (B1 Type).

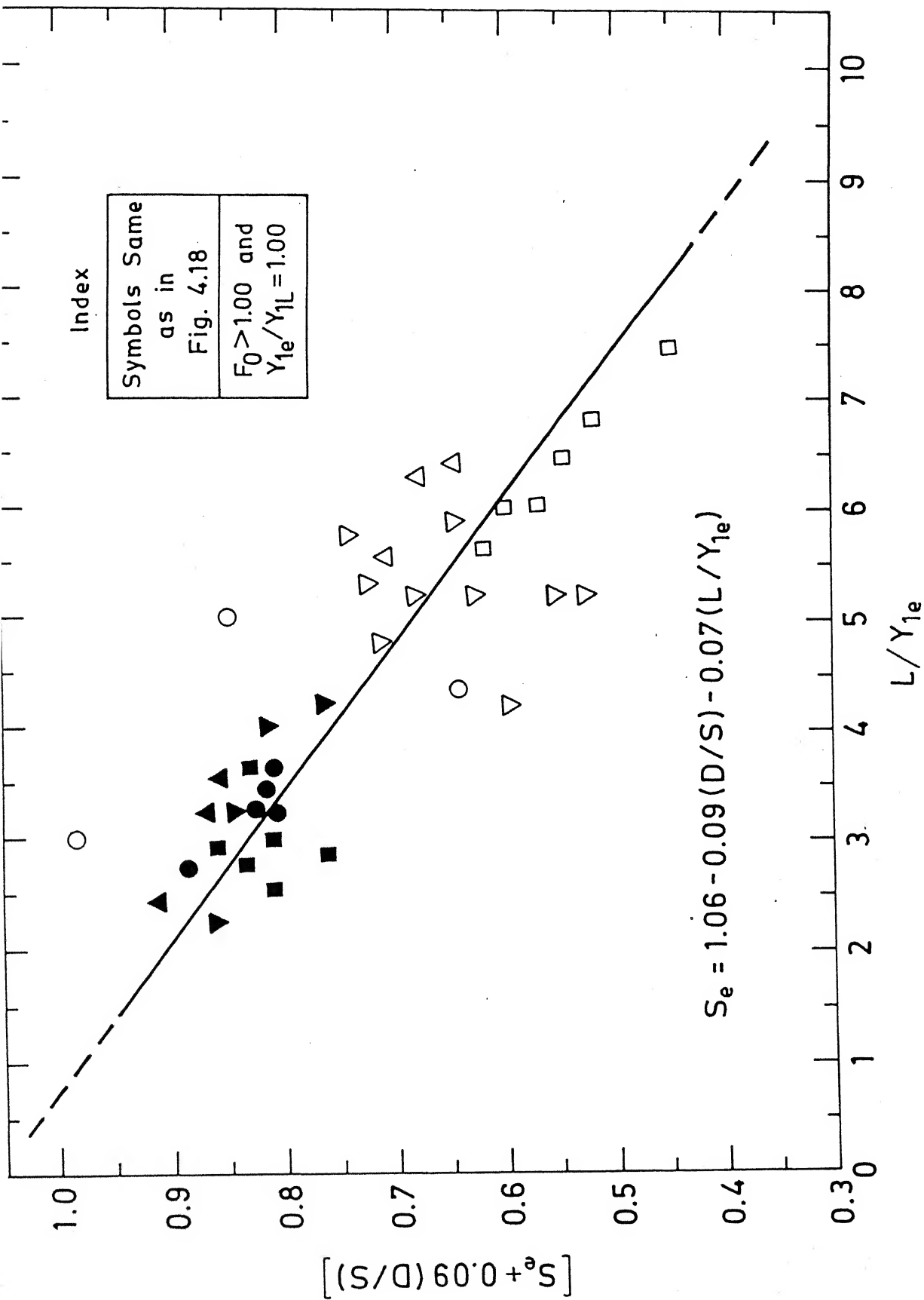


Fig. 4.19. Variation of Energy-slope Over the Rack in Super-

$$S_e = 1.06 - 0.09 (D/S) - 0.075 (L/y_{1e}) \quad (4.38)$$

This is shown in Fig. 4.19 where $[S_e + 0.09 (D/S)]$ is plotted against L/y_{1e} and all the data on Bl flows are plotted. Eq. (4.38) is also shown. The maximum scatter of data is about 20% while the average scatter is roughly 8%. Hence, the equation (4.38) can satisfactorily be used for the estimation of the energy slope in Bl flows.

It is interesting to see that the coefficient of D/S in both the Eqns. (4.36) and (4.38) is same at 0.09. The energy slope, S_e is smaller in Al flows, where the approach flow was subcritical, when compared to Bl flows. The range of parameters F_o, F_1, F_2 and L/y_{1e} used in the study are shown in Table 4.1.

Table 4.1 Range of Parameters used in the Study of S_e

Type of flow	F_o	$F_1 = \frac{V_1}{\sqrt{gy_{1e}}}$	$F_2 = \frac{V_2}{\sqrt{gy_{2e}}}$	L/y_{1e}
Al	0.60-0.85	1.1 - 1.5	1.1-1.45	0.67-2.10
Bl	1.3 -5.4	1.6 - 6.1	4.8-6.5	2.0-8.0

It is obvious from the Table 4.1 that in Al flows, the inlet Froude number F_1 varies in a very small range (1.1-1.5) and the range of flows F_1 through F_2 is also small. However, in Bl flow high Froude numbers as much as 6.5 were encountered

and account for higher energy losses. The Eqs.(4.36) and (4.38) must be considered as only approximate relationship. However, they underscore the magnitude of E_L and their use is definitely an improvement over the assumption of zero energy loss.

4.4.4 Energy loss in A3 Flows:

The analysis of all experimental data on A3 flows shows that the percentage energy loss ($\frac{E_L}{E_1}$) for most of the data lies within 2 to 4%. Also, the energy slope (S_e) for mighty percent of data ranged from 0.05 to 0.15. The range of energy loss and the pertinent parameters of the flow observed in the study of A3 flows are shown in Table 4.2.

Table 4.2 Range of Energy Loss Parameters in A3 Flows:

Parameters	Range		
	Min.	Max	Average
$\frac{E_L}{E_1} \%$	0.0	10.0	3.5
S_e	0.0	0.22	0.09
L/y_{1e}	0.15	0.90	0.40
S_b	0.10	0.55	0.25

The range of E_L/E_1 shown in Table 4.2 is quite small and no distinct variation of $\frac{E_L}{E_1}$ or S_e could be observed with $\frac{L}{y_{1e}}$ and other parameters. More over, it is clear from

Table 4.2 that the energy loss $\frac{E_L}{E_1}$ as well as energy slope S_e are quite small. An average value for whole the data observed is given in the table with a view to show that majority of data were well within 2 to 4% energy loss.

Hence, for the analysis of A3 flows, the energy loss over the rack for $S_b \leq 0.55$ can be taken as negligible for practical purposes.

4.5 Water Surface Profile Calculations:

In view of the above analysis, it is obvious that the energy loss over the rack particularly in A1 and B1 flows can not be neglected. As such, Equations (2.4) and (2.12) suggested by Mostkow for water surface profile calculations along the rack by assuming constant specific energy all along it, are not justified to use.

The original equation of SVF with decreasing discharge for a rectangular, prismatic and horizontal channel by taking kinetic energy correction factor $\alpha=1.0$, can be represented as

$$\frac{dy}{dx} = \frac{-S_e - \frac{Q_D q_*}{g B^2 y^2}}{1 - \frac{Q_D^2}{g B^2 y^3}} \quad (4.39)$$

where S_e = Energy slope over rack; Q_D = Diverted flow through the rack ;

and q_* = discharge per unit length of the rack and can be defined as

$$q_* = \frac{Q_D}{L} = C_d B \sqrt{2gE_o} = \text{Constant} \quad (4.40)$$

C_d can be calculated from equation (4.12) or (4.17) depending upon the type of flow A1 or B1 respectively.

S_e can be calculated from equation (4.36) or (4.38) depending upon the type of flow.

Then, the Eq. (4.39), after substituting the values of S_e and q_* , can be solved by a suitable numerical technique to obtain the water surface profile over the rack. Since, the energy loss in A3 flows, is negligibly small, Mostkow equations (2.4) and 2.12) can be used for water surface profile determination in this particular case.

CHAPTER V

CONCLUSIONS AND RECOMMENDATIONS

5.1 Conclusions:

A detailed experimental study has been made on the hydraulic behaviour of horizontal longitudinal bar bottom-racks, made of circular bars, in A1, A3 and B1 flows. Based on the study the following conclusions are drawn.

1. The variation of the limiting inlet depth ratio $\frac{y_{1L}}{y_c}$ has been studied for A1 and B1 flows separately. In A1 flows it is found that $\frac{y_{1L}}{y_c}$ varies with the opening area ratio ϵ and is not affected by B/L ratio of the rack, while in B1 flows $\frac{y_{1L}}{y_c}$ depends upon the Froude number of approach flow F_o as well as ϵ .
2. A coefficient of discharge C_d is defined as $C_d = \frac{Q_D}{BL\epsilon\sqrt{2gE_o}}$. Variation of C_d has been studied in A1, A3 and B1 flows separately. It is observed that C_d is a function of $\frac{v_o^2}{2gE_o}$ and D/S ratio of the rack in all the three types of flows studied. The effect of B/L on C_d is found to be insignificant. The effect of the flow parameter $\frac{v_o^2}{2gE_o}$ is found to be negligible in A1 flows while it has a pronounced effect in B1 flows. The best fit Eqs. (4.12), (4.15) and (4.17) have been obtained for

estimation of C_d in A1, A3 and B1 flows respectively. It is found that the value of C_d in B1 flows for a given flow and rack parameter is higher than the corresponding value in A1 flows. Also, C_d in A3 flows is higher than that in A1 flows. A1 and A3 flow over the limiting case of a rack (viz, a slot) are also studied.

3. The diversion ratio $\frac{Q_D}{Q_S}$ is found to be a function of $\frac{L}{Y_c}$ and $\frac{D}{S}$ for A1 and B1 flows. It is observed that the value of $\frac{Q_D}{Q_S}$ is higher in A1 flows than for corresponding value in B1 flows. The variation of the diversion ratio in A1 and B1 flows are expressed by Eqs (4.25) and (4.28) respectively. The minimum length of the rack required for the whole diversion of the incoming flow has also been obtained from these equations.
4. For a slot in A1 flows the diversion ratio is related with $\frac{L}{Y_c}$ by a simple equation (Eq. 4.30).
5. An attempt has been made for the determination of the energy loss over the rack. An average value of percentage energy loss with respect to inlet specific energy is determined as 15% and 30% in A1 and B1 flows respectively. It is also observed that energy loss in A3 flows can be taken as essentially zero. The variation of S_e has been studied with $\frac{L}{Y_{1e}}$ and $\frac{D}{S}$ for both A1 and B1 flows separately. It is found that the value of S_e in B1 flows is higher than the corresponding value in A1.

flows. Best fit equations (4.36) and (4.38) have been determined for estimating the energy slope S_e in A1 and B1 flows separately.

6. In view of substantial energy losses, use of Mostkow equations for water surface profile determination, based on the assumption of zero energy loss seems to be erroneous. As such, using the energy slope S_e calculated from corresponding equations obtained in the present study, in the original equation of SVF with decreasing discharge and solving it by any suitable numerical method, is the suggested approach for the determination of water surface profile over the rack. However the Mostkow equations can be used for determining water surface profiles in A3 flows without much error because of the negligible energy loss in this flow case.
7. Information of this study is useful in the design of trench weir intakes. A simple fortran program has been given in appendix II for determining the length of such trench weirs and compared with their original recommended design.

5.2 Recommendations:

Based on the literature review and the present study, the following further studies on this topic are recommended.

1. Inclined longitudinal bar bottom-racks need to be studied.
2. The study could be extended to the perforated plate bottom-racks also.
3. Study could be extended for other shapes of bars namely Rectangular, stream lined etc to obtain efficient and economical bar geometry.
4. A more detailed study is needed for energy loss determination over the rack.

LIST OF REFERENCES

1. Chow, V.T., 'Open Channel Hydraulics', McGraw Hill, New York, pp 337-340, 1959.
2. Dhillon, G.S., 'Hydraulics of Bottom-Intakes' Indian Jl. of Power and River valley Dev., pp 243-250, Oct. 1986.
3. Mostkow, M.A., 'A Theoretical Study of Bottom Type Water Intakes', La Houille Blanche, No. 4; pp 570-580, Sept. 1957.
4. Nasser, M.S., Venkataraman, P. and Ramamurthy, A.S., 'Flow in a Channel with a Slot in the Bed.' Jl. of Hyd. Res., No.4, pp 359-367, 1980.
5. Nosedá, G. 'Operation and Design of Bottom Intake Racks', Proc. 6th General Meeting Int. Assoc. Hyd. Res., 3 (C 17) 1-11, 1956.
6. Ramamurthy, A.S. and Satish, M.G., 'Discharge Characteristics of Flow Past a Floor Slot', Jl. of Irrig. and Drain. Engg., Vol. 112, No. 1, ASCE, pp 20-27 Feb 1986.
7. Rangaraju, K.G., Asawa, G.L., and Seetharamaiah R. 'Analysis of Flow Through Bottom-Racks in Open Channels' pp 237-240, Dec. 1977. (Fluid Mech. Conf. Adelaide, Australia).
8. Sengupta, D., 'Hydraulic Behaviour of Bottom-Racks', M. Tech. Thesis, Indian Institute of Technology, Kanpur, Civil Engg. Dept., Aug. 1971.
9. Singh, R. and Mahajan, S.K., 'Hydraulic Design of a Trench Weir', Proc. 52nd Annual R and D Session, CII, Pub. No. 176, Vol.1, pp 289-304, Feb. 1985.

10. Subramanya, K., 'Flow in Open Channels', Tata McGraw Hill Pub. Co. Ltd., New Delhi, India, 1986.
11. Venkataraman, P., 'Discharge Characteristics of an Idealised Bottom-Intake', Jl. of Inst. of Eng. (India), Vol.58, Pts CI2 and 3, pp 99, Sept. Nov. 1977.
12. Venkataraman, P., Nasser, M.S. and Ramamurthy, A.S., 'Flow Behaviour in Power Channels With Bottom Diversion Works', Proc. 18th Cong. of IAHR, Vol. 4, pp 115-122, Sept. 10-14, 1979.
13. Venkataraman, P., 'Behaviour of Flow in Channels with Bottom Openings', Jl. of Inst. of Eng. (India), Vol 61, pp 87-90, Sept. 1980.
14. White, J.K., Charlton, J.A. and Ramsay, C.A.W., 'On the Design of Bottom-Intakes for Diverting Stream Flows', Proc. of Inst. of Civil Eng., London, Vol 51, pp.337-345, Feb. 1972.

APPENDIX I
TABLE I A (BASIC DATA)

EXP. NO	EPS	R (m)	L (m)	D/S	QS (cume/s)	QD (cume/s)	YD (m)	r1 ² (m)	Y2e (m)	T (°C)	$\frac{r_1^2}{C} \left(\frac{m^2}{s} \right)$
1	0.48	0.15	.075	1.17	0.01038	0.00475	0.095	0.003	0.040	27.8	0.05E-06
2	0.48	0.15	.075	1.17	0.00421	0.00370	0.054	0.036	0.013	27.8	0.05E-06
3	0.48	0.15	.075	1.17	0.00998	0.00475	0.094	0.002	0.042	27.8	0.05E-06
4	0.48	0.15	.075	1.17	0.01368	0.00510	0.116	0.016	0.058	27.8	0.05E-06
5	0.48	0.15	.075	1.17	0.00674	0.00421	0.072	0.048	0.025	27.8	0.05E-06
6	0.48	0.15	.075	1.17	0.00914	0.00453	0.088	0.058	0.036	27.8	0.05E-06
7	0.48	0.15	.075	1.17	0.01458	0.00534	0.116	0.078	0.058	27.8	0.05E-06
8	0.48	0.15	.075	1.17	0.00407	0.00350	0.056	0.038	0.017	27.8	0.05E-06
9	0.48	0.15	.075	1.17	0.00669	0.00410	0.066	0.044	0.050	27.8	0.05E-06
10	0.48	0.15	.075	1.17	0.00976	0.00559	0.094	0.084	0.090	27.8	0.05E-06
11	0.48	0.15	.075	1.17	0.01119	0.00605	0.108	0.102	0.114	27.8	0.05E-06
12	0.48	0.15	.075	1.17	0.01250	0.00702	0.128	0.126	0.132	27.8	0.05E-06
13	0.36	0.15	.075	1.89	0.00820	0.00370	0.094	0.000	0.042	27.8	0.05E-06
14	0.36	0.15	.075	1.89	0.00868	0.00370	0.090	0.000	0.040	27.8	0.05E-06
15	0.36	0.15	.075	1.89	0.00610	0.00309	0.066	0.044	0.020	27.8	0.05E-06
16	0.36	0.15	.075	1.89	0.01085	0.00400	0.096	0.065	0.044	27.8	0.05E-06
17	0.36	0.15	.075	1.89	0.01240	0.00410	0.104	0.072	0.050	27.8	0.05E-06
18	0.36	0.15	.075	1.89	0.00485	0.00291	0.058	0.038	0.014	27.8	0.05E-06
19	0.36	0.15	.075	1.89	0.01447	0.00534	0.128	0.112	0.120	27.8	0.05E-06
20	0.36	0.15	.075	1.89	0.01568	0.00534	0.132	0.115	0.124	27.8	0.05E-06
21	0.24	0.15	.075	3.33	0.00248	0.00177	0.038	0.025	0.010	22.0	0.05E-06

22	0.24	0.15	.075	3.33	0.06391	0.00200	0.048	0.035	0.014	22.0	0.95E-06
23	0.24	0.15	.075	3.33	0.06537	0.00227	0.060	0.042	0.020	22.0	0.95E-06
24	0.24	0.15	.075	3.33	0.06577	0.00237	0.064	0.044	0.022	22.0	0.95E-06
25	0.24	0.15	.075	3.33	0.06765	0.00340	0.092	0.064	0.088	22.0	0.95E-06
26	0.24	0.15	.075	3.33	0.06920	0.00400	0.128	0.120	0.120	22.0	0.95E-06
27	0.24	0.15	.075	3.33	0.01189	0.00486	0.186	0.174	0.174	22.0	0.95E-06
28	0.24	0.15	.075	3.33	0.01348	0.00534	0.224	0.208	0.208	22.0	0.95E-06
29	0.16	0.15	.075	5.50	0.00505	0.00147	0.056	0.045	0.030	22.0	0.95E-06
30	0.16	0.15	.075	5.50	0.01027	0.00197	0.098	0.071	0.054	22.0	0.95E-06
31	0.16	0.15	.075	5.50	0.00709	0.00171	0.076	0.056	0.038	22.0	0.95E-06
32	0.16	0.15	.075	5.50	0.00926	0.00184	0.088	0.066	0.050	22.0	0.95E-06
33	0.16	0.15	.075	5.50	0.00861	0.00177	0.086	0.062	0.050	22.0	0.95E-06
34	0.16	0.15	.075	5.50	0.01477	0.00340	0.192	0.184	0.184	22.0	0.95E-06
35	0.16	0.15	.075	5.50	0.01198	0.00279	0.138	0.129	0.138	22.0	0.95E-06
36	0.16	0.15	.075	5.50	0.01381	0.00322	0.180	0.174	0.176	22.0	0.95E-06
37	0.16	0.15	.075	5.50	0.00960	0.00214	0.092	0.072	0.078	22.0	0.95E-06
38	0.16	0.15	.075	5.50	0.01052	0.00239	0.108	0.095	0.100	22.0	0.95E-06
39	0.16	0.15	.075	5.50	0.01682	0.00340	0.235	0.224	0.224	22.0	0.95E-06
40	0.16	0.15	.038	5.50	0.00552	0.00076	0.064	0.046	0.040	24.0	0.95E-06
41	0.16	0.15	.038	5.50	0.00283	0.00062	0.040	0.030	0.020	24.0	0.95E-06
42	0.16	0.15	.038	5.50	0.00159	0.00055	0.030	0.020	0.010	24.0	0.95E-06
43	0.16	0.15	.038	5.50	0.00720	0.00090	0.078	0.056	0.050	24.0	0.95E-06
44	0.16	0.15	.038	5.50	0.00998	0.00131	0.134	0.126	0.130	24.0	0.95E-06
45	0.16	0.15	.038	5.50	0.01331	0.00165	0.206	0.196	0.196	24.0	0.95E-06
46	0.16	0.15	.038	5.50	0.01514	0.00184	0.232	0.232	0.232	24.0	0.95E-06

47	0.10	0.15	.038	5.50	0.01568	0.00184	0.246	0.246	0.246	0.246	0.91E-06
48	0.24	0.15	.038	3.33	0.00140	0.00076	0.026	0.018	0.014	22.0	0.95E-06
49	0.24	0.15	.038	3.33	0.00222	0.00084	0.034	0.024	0.016	22.0	0.95E-06
50	0.24	0.15	.038	3.33	0.00271	0.00090	0.040	0.027	0.018	22.0	0.95E-06
51	0.24	0.15	.038	3.33	0.00330	0.00097	0.044	0.031	0.022	22.0	0.95E-06
52	0.24	0.15	.038	3.33	0.00476	0.00145	0.080	0.078	0.078	22.0	0.95E-06
53	0.24	0.15	.038	3.33	0.00628	0.00184	0.120	0.112	0.112	22.0	0.95E-06
54	0.24	0.15	.038	3.33	0.00824	0.00221	0.172	0.164	0.164	22.0	0.95E-06
55	0.24	0.15	.038	3.33	0.01051	0.00267	0.230	0.220	0.220	22.0	0.95E-06
56	0.36	0.15	.038	1.89	0.00204	0.00111	0.034	0.022	0.010	24.0	0.91E-06
57	0.36	0.15	.038	1.89	0.00568	0.00153	0.062	0.042	0.030	24.0	0.91E-06
58	0.36	0.15	.038	1.89	0.00145	0.00111	0.030	0.018	0.008	24.0	0.91E-06
59	0.36	0.15	.038	1.89	0.00310	0.00136	0.044	0.030	0.020	24.0	0.91E-06
60	0.36	0.15	.038	1.89	0.00472	0.00153	0.058	0.040	0.030	24.0	0.91E-06
61	0.36	0.15	.038	1.89	0.00636	0.00171	0.070	0.046	0.040	24.0	0.91E-06
62	0.36	0.15	.038	1.89	0.00381	0.00142	0.050	0.034	0.024	24.0	0.91E-06
63	0.36	0.15	.038	1.89	0.00769	0.00207	0.082	0.066	0.088	24.0	0.91E-06
64	0.36	0.15	.038	1.89	0.00967	0.00271	0.130	0.126	0.130	24.0	0.91E-06
65	0.36	0.15	.038	1.89	0.01204	0.00322	0.178	0.168	0.172	24.0	0.91E-06
66	0.36	0.15	.038	1.89	0.01378	0.00350	0.209	0.200	0.200	24.0	0.91E-06
67	0.48	0.15	.038	1.17	0.00629	0.00190	0.066	0.044	0.036	22.0	0.95E-06
68	0.48	0.15	.038	1.17	0.00709	0.00200	0.074	0.048	0.042	22.0	0.95E-06
69	0.48	0.15	.038	1.17	0.00300	0.00153	0.044	0.028	0.014	22.0	0.95E-06
70	0.48	0.15	.038	1.17	0.00795	0.00247	0.084	0.076	0.086	22.0	0.95E-06
71	0.48	0.15	.038	1.17	0.01018	0.00313	0.134	0.132	0.134	22.0	0.95E-06

72	0.48	0.15	.036	1.17	0.01228	0.00370	0.178	0.110	0.172	22.0	0.95E-06
73	0.48	0.15	.038	1.17	0.01384	0.00400	0.212	0.204	0.204	22.0	0.95E-06
74	0.48	0.15	.038	1.17	0.01522	0.00415	0.240	0.232	0.232	22.0	0.95E-06
75	1.00	0.15	.038	0.00	0.00261	0.00218	0.038	0.022	0.010	22.0	0.95E-06
76	1.00	0.15	.038	0.00	0.00458	0.00251	0.054	0.044	0.018	22.0	0.95E-06
77	1.00	0.15	.038	0.00	0.00624	0.00271	0.064	0.040	0.022	22.0	0.95E-06
78	1.00	0.15	.030	0.00	0.00159	0.00159	0.028	0.016	0.008	22.0	0.95E-06
79	1.00	0.15	.038	0.00	0.00363	0.00236	0.046	0.026	0.013	22.0	0.95E-06
80	1.00	0.15	.038	0.00	0.00761	0.00390	0.078	0.064	0.070	22.0	0.95E-06
81	1.00	0.15	.038	0.00	0.00911	0.00487	0.096	0.046	0.096	22.0	0.95E-06
82	1.00	0.15	.038	0.00	0.01055	0.00565	0.119	0.114	0.114	22.0	0.95E-06
83	1.00	0.15	.038	0.00	0.01309	0.00702	0.164	0.160	0.160	22.0	0.95E-06
84	1.00	0.15	.055	0.00	0.00296	0.00296	0.038	0.024	0.002	22.0	0.95E-06
85	1.00	0.15	.075	0.00	0.00578	0.00442	0.060	0.036	0.008	22.0	0.95E-06
86	1.00	0.15	.075	0.00	0.00776	0.00476	0.072	0.046	0.020	22.0	0.95E-06
87	1.00	0.15	.075	0.00	0.00920	0.00499	0.082	0.052	0.026	22.0	0.95E-06
88	1.00	0.15	.075	0.00	0.01071	0.00637	0.094	0.064	0.074	22.0	0.95E-06
89	1.00	0.15	.075	0.00	0.01267	0.00888	0.108	0.092	0.096	22.0	0.95E-06
90	1.00	0.15	.075	0.00	0.01416	0.00974	0.118	0.098	0.098	22.0	0.95E-06
91	1.00	0.15	.075	0.00	0.01507	0.01043	0.126	0.116	0.120	22.0	0.95E-06
92	0.49	0.60	.170	1.13	0.04660	0.04660	0.060	0.051	0.001	30.0	0.81E-06
93	0.49	0.60	.300	1.13	0.09100	0.07370	0.080	0.076	0.018	30.0	0.81E-06
94	0.49	0.60	.300	1.13	0.09510	0.05830	0.058	0.058	0.036	30.0	0.81E-06
95	0.34	0.60	.300	2.05	0.05670	0.05100	0.052	0.052	0.005	29.0	0.81E-06
96	0.34	0.60	.300	2.05	0.08020	0.05160	0.054	0.054	0.025	29.0	0.81E-06

97	0.34	0.60	.300	2.05	0.07380	0.05270	0.056	0.056	0.017	29.0	0.81E-06
98	0.34	0.60	.300	2.05	0.05570	0.04870	0.042	0.042	0.016	29.0	0.81E-06
99	0.34	0.60	.300	2.05	0.05510	0.05090	0.044	0.044	0.005	29.0	0.81E-06
100	0.27	0.60	.300	2.90	0.05180	0.03980	0.045	0.045	0.012	27.8	0.85E-06
101	0.27	0.60	.300	2.90	0.06960	0.04110	0.050	0.050	0.024	27.8	0.85E-06
102	0.27	0.60	.300	2.90	0.07370	0.04110	0.042	0.042	0.026	27.8	0.85E-06
103	0.27	0.60	.300	2.90	0.07620	0.04110	0.040	0.040	0.019	27.8	0.85E-06
104	0.27	0.60	.300	2.90	0.07810	0.04110	0.039	0.039	0.021	27.8	0.85E-06
105	0.27	0.60	.300	2.90	0.06317	0.04640	0.052	0.052	0.014	27.8	0.85E-06
106	0.27	0.60	.300	2.90	0.07284	0.04552	0.059	0.059	0.021	27.8	0.85E-06
107	0.27	0.60	.300	2.90	0.05343	0.04596	0.057	0.057	0.010	27.8	0.85E-06
108	0.16	0.60	.300	5.61	0.04100	0.03200	0.064	0.064	0.010	22.0	0.95E-06
109	0.16	0.60	.300	5.61	0.04889	0.03290	0.060	0.060	0.018	22.0	0.95E-06
110	0.16	0.60	.300	5.61	0.05548	0.03370	0.060	0.060	0.022	22.0	0.95E-06
111	0.16	0.60	.300	5.61	0.05050	0.03284	0.058	0.058	0.023	22.0	0.95E-06
112	0.16	0.60	.300	5.61	0.06310	0.03490	0.062	0.062	0.028	22.0	0.95E-06
113	0.16	0.60	.300	5.61	0.07190	0.03490	0.063	0.063	0.036	22.0	0.95E-06
114	0.16	0.60	.300	5.61	0.07890	0.03533	0.060	0.060	0.036	22.0	0.95E-06
115	0.16	0.60	.300	5.61	0.08120	0.03542	0.056	0.056	0.033	22.0	0.95E-06
116	0.16	0.60	.300	5.61	0.08261	0.03626	0.073	0.073	0.040	22.0	0.95E-06
117	0.16	0.60	.300	5.61	0.05287	0.03250	0.060	0.060	0.020	22.0	0.95E-06
118	0.16	0.60	.150	5.61	0.02875	0.01674	0.043	0.043	0.024	24.0	0.91E-06
119	0.16	0.60	.150	5.61	0.04163	0.01692	0.044	0.044	0.023	24.0	0.91E-06
120	0.16	0.60	.150	5.61	0.04500	0.01702	0.042	0.042	0.026	24.0	0.91E-06
121	0.16	0.60	.150	5.61	0.05821	0.01799	0.049	0.049	0.040	24.0	0.91E-06

122	0.16	0.60	.150	5.61	0.05346	0.01799	0.052	0.046	0.034	24.0	0.91E-06
123	0.16	0.60	.150	5.61	0.07396	0.01980	0.056	0.064	0.030	24.0	0.91E-06
125	0.16	0.60	.150	5.61	0.07310	0.01943	0.052	0.066	0.056	24.0	0.91E-06
125	0.27	0.60	.150	2.90	0.05133	0.02508	0.054	0.044	0.028	24.0	0.91E-06
126	0.27	0.60	.150	2.90	0.03549	0.02408	0.048	0.038	0.016	24.0	0.91E-06
127	0.27	0.60	.150	2.90	0.06388	0.02528	0.064	0.054	0.039	24.0	0.91E-06
128	0.27	0.60	.150	2.90	0.06771	0.02412	0.058	0.056	0.042	24.0	0.91E-06
129	0.27	0.60	.150	2.90	0.07370	0.02316	0.056	0.054	0.046	24.0	0.91E-06
129	0.27	0.60	.150	2.90	0.07891	0.02278	0.060	0.052	0.042	24.0	0.91E-06
130	0.27	0.60	.150	2.90	0.08056	0.02241	0.056	0.055	0.046	24.0	0.91E-06
132	0.34	0.60	.150	2.05	0.04350	0.02727	0.050	0.044	0.022	24.0	0.91E-06
133	0.34	0.60	.150	2.05	0.05816	0.02431	0.048	0.040	0.030	24.0	0.91E-06
134	0.34	0.60	.150	2.05	0.06774	0.02241	0.050	0.050	0.042	24.0	0.91E-06
135	0.34	0.60	.150	2.05	0.07486	0.03084	0.070	0.060	0.042	24.0	0.91E-06
136	0.34	0.60	.150	2.05	0.07968	0.02982	0.072	0.072	0.050	24.0	0.91E-06
137	0.34	0.60	.150	2.05	0.08194	0.03392	0.086	0.080	0.052	24.0	0.91E-06
138	0.49	0.60	.150	1.13	0.05146	0.03084	0.054	0.046	0.026	22.0	0.95E-06
139	0.49	0.60	.150	1.13	0.06103	0.02854	0.052	0.048	0.033	22.0	0.95E-06
141	0.49	0.60	.150	1.13	0.06686	0.02684	0.052	0.046	0.033	22.0	0.95E-06
142	0.49	0.60	.150	1.13	0.07253	0.02586	0.058	0.050	0.037	22.0	0.95E-06
143	0.49	0.60	.150	1.13	0.07851	0.02469	0.054	0.054	0.047	22.0	0.95E-06

EXPS. 144 TO 146 FOR VELOCITY PROFILE ONLY.

TABLE 16 (DERIVED DATA)

EXP. NO	EPS	D/S	F0	(V0**2/2qF0)	Cd	QD/QS	Se	u/1C	u/11e	u20
1	0.48	1.17	0.75	0.222	0.568	0.458	0.526	0.95	1.19	0.91E+05
2	0.48	1.17	0.71	0.203	0.594	0.879	0.673	1.14	2.06	0.33E+05
3	0.48	1.17	0.74	0.214	0.574	0.476	0.581	0.98	1.21	0.73E+05
4	0.48	1.17	0.74	0.214	0.555	0.373	0.556	0.19	0.99	0.11E+05
5	0.48	1.17	0.74	0.216	0.580	0.624	0.592	1.27	1.50	0.53E+05
6	0.48	1.17	0.75	0.217	0.565	0.496	0.548	1.04	1.29	0.72E+05
7	0.48	1.17	0.79	0.236	0.573	0.367	0.556	0.16	0.90	0.11E+05
8	0.48	1.17	0.75	0.220	0.547	0.750	0.517	1.02	1.97	0.37E+05
9	0.48	1.17	0.84	0.261	0.574	0.613	0.537	1.28	1.70	0.52E+05
10	0.48	1.17	0.72	0.206	0.679	0.573	0.263	0.99	0.89	0.77E+05
11	0.48	1.17	0.67	0.184	0.764	0.594	0.156	0.91	0.74	0.83E+05
12	0.48	1.17	0.58	0.144	0.759	0.562	0.165	0.84	0.60	0.93E+05
13	0.36	1.89	0.61	0.155	0.618	0.451	0.457	1.11	1.25	0.64E+05
14	0.36	1.89	0.68	0.190	0.616	0.426	0.430	1.07	1.25	0.63E+05
15	0.36	1.89	0.77	0.226	0.589	0.506	0.216	1.46	1.70	0.43E+05
16	0.36	1.89	0.78	0.232	0.630	0.368	0.389	0.92	1.15	0.83E+05
17	0.36	1.89	0.79	0.236	0.619	0.331	0.357	0.85	1.04	0.97E+05
18	0.36	1.89	0.74	0.215	0.598	0.601	0.234	1.58	1.97	0.38E+05
19	0.36	1.89	0.67	0.184	0.752	0.369	0.273	0.76	0.67	0.11E+05
20	0.36	1.89	0.70	0.195	0.736	0.341	0.232	0.12	0.65	0.12E+05
21	0.24	3.33	0.71	0.203	0.679	0.714	0.345	2.47	3.00	0.17E+05

22	0.24	3.33	0.73	0.239	0.660	0.511	0.094	1.03	2.14	0.27E+05
23	0.24	3.33	0.76	0.232	0.680	0.424	0.064	1.48	1.73	0.33E+05
24	0.24	3.33	0.76	0.223	0.690	0.411	0.091	1.41	1.70	0.40E+05
25	0.24	3.33	0.58	0.145	0.660	0.445	0.127	1.17	0.89	0.54E+05
26	0.24	3.33	0.43	0.084	0.894	0.435	0.121	1.03	0.63	0.65E+05
27	0.24	3.33	0.32	0.047	0.920	0.409	0.092	0.07	0.43	0.83E+05
28	0.24	3.33	0.27	0.035	0.927	0.396	0.081	0.00	0.36	0.95E+05
29	0.16	5.50	0.81	0.248	0.677	0.292	0.151	1.54	1.67	0.35E+05
30	0.16	5.50	0.71	0.202	0.704	0.192	0.145	0.96	1.00	0.72E+05
31	0.16	5.50	0.72	0.206	0.693	0.241	0.119	1.43	1.34	0.50E+05
32	0.16	5.50	0.76	0.222	0.685	0.198	0.142	1.03	1.14	0.55E+05
33	0.16	5.50	0.73	0.209	0.674	0.206	0.178	1.08	1.21	0.60E+05
34	0.16	5.50	0.37	0.065	0.941	0.230	0.079	0.75	0.41	0.10E+05
35	0.16	5.50	0.50	0.110	0.888	0.233	0.007	0.87	0.58	0.84E+05
36	0.16	5.50	0.38	0.069	0.918	0.233	0.054	0.79	0.43	0.07E+05
37	0.16	5.50	0.74	0.215	0.784	0.221	0.184	1.00	1.04	0.63E+05
38	0.16	5.50	0.63	0.165	0.835	0.228	0.104	0.94	0.79	0.74E+05
39	0.16	5.50	0.31	0.047	0.859	0.202	0.062	0.09	0.33	0.12E+05
40	0.16	5.50	0.73	0.208	0.672	0.138	0.175	0.73	0.82	0.40E+05
41	0.16	5.50	0.75	0.221	0.684	0.218	0.065	1.13	1.25	0.21E+05
42	0.16	5.50	0.65	0.175	0.726	0.347	-0.002	1.66	1.88	0.12E+05
43	0.16	5.50	0.70	0.198	0.727	0.126	0.201	0.01	0.67	0.53E+05
44	0.16	5.50	0.43	0.086	0.858	0.131	0.004	0.49	0.30	0.73E+05
45	0.16	5.50	0.30	0.044	0.891	0.124	0.065	0.40	0.19	0.03E+05
46	0.16	5.50	0.29	0.040	0.937	0.121	0.059	0.37	0.16	0.11E+05

47	0.16	5.59	0.27	0.036	0.914	0.117	0.054	0.36	0.15	0.11E+00
48	0.24	3.33	0.71	0.201	0.706	0.545	0.340	1.01	2.08	0.94E+04
50	0.24	3.33	0.75	0.221	0.674	0.380	0.283	1.33	1.50	0.10E+05
51	0.24	3.33	0.72	0.206	0.673	0.334	0.241	1.17	1.39	0.19E+05
52	0.24	3.33	0.70	0.224	0.681	0.294	0.247	1.02	1.21	0.23E+05
53	0.24	3.33	0.45	0.091	0.814	0.303	0.110	0.80	0.48	0.33E+05
54	0.24	3.33	0.32	0.049	0.864	0.292	0.095	0.07	0.33	0.44E+05
55	0.24	3.33	0.25	0.029	0.878	0.268	0.071	0.56	0.23	0.58E+05
56	0.24	3.33	0.20	0.020	0.921	0.254	0.061	0.47	0.17	0.74E+05
57	0.36	1.89	0.69	0.193	0.601	0.544	0.317	1.41	1.70	0.15E+05
58	0.36	1.89	0.78	0.235	0.599	0.269	0.269	0.71	0.89	0.42E+05
59	0.36	1.89	0.59	0.150	0.657	0.703	0.548	1.77	2.08	0.11E+05
60	0.36	1.89	0.71	0.203	0.645	0.439	0.455	1.07	1.25	0.23E+05
61	0.36	1.89	0.72	0.205	0.631	0.324	0.425	0.61	0.94	0.35E+05
62	0.36	1.89	0.73	0.211	0.640	0.269	0.498	0.06	0.82	0.47E+05
63	0.36	1.89	0.73	0.209	0.628	0.372	0.424	0.93	1.10	0.28E+05
64	0.36	1.89	0.70	0.195	0.723	0.269	-0.013	0.58	0.57	0.50E+05
65	0.36	1.89	0.44	0.088	0.800	0.230	0.076	0.50	0.30	0.71E+05
66	0.36	1.89	0.34	0.055	0.827	0.267	0.045	0.43	0.22	0.83E+05
67	0.36	1.89	0.31	0.046	0.837	0.254	0.127	0.39	0.19	0.10E+05
68	0.48	1.17	0.79	0.238	0.541	0.302	0.550	0.07	0.85	0.44E+05
69	0.48	1.17	0.75	0.219	0.544	0.283	0.592	0.01	0.78	0.50E+05
70	0.48	1.17	0.69	0.193	0.548	0.510	0.402	1.09	1.34	0.21E+05
71	0.48	1.17	0.69	0.194	0.640	0.311	0.149	0.57	0.49	0.50E+05
72	0.48	1.17	0.44	0.089	0.682	0.307	0.139	0.48	0.28	0.71E+05

73	0.48	1.17	0.35	0.057	0.711	0.301	0.111	0.43	0.22	0.85E+05
74	0.48	1.17	0.39	0.044	0.710	0.289	0.137	0.37	0.13	0.77E+05
75	0.48	1.17	0.28	0.037	0.690	0.273	0.123	0.37	0.10	0.11E+06
76	1.00	0.00	0.75	0.220	0.396	0.833	1.050	1.20	1.70	0.13E+05
77	1.00	0.00	0.78	0.232	0.380	0.548	0.724	0.62	1.10	0.32E+05
78	1.00	0.00	0.82	0.252	0.372	0.434	0.391	0.07	0.94	0.44E+05
79	1.00	0.00	0.72	0.206	0.424	1.000	1.010	1.33	1.88	0.11E+05
80	1.00	0.00	0.78	0.234	0.386	0.650	0.940	0.26	1.44	0.25E+05
81	1.00	0.00	0.74	0.216	0.495	0.512	0.524	0.59	0.59	0.53E+05
82	1.00	0.00	0.65	0.175	0.573	0.535	0.420	0.52	0.39	0.64E+05
83	1.00	0.00	0.55	0.130	0.614	0.536	0.400	0.47	0.33	0.74E+05
84	1.00	0.00	0.42	0.081	0.667	0.537	0.318	0.41	0.23	0.92E+05
85	1.00	0.00	0.85	0.265	0.356	1.000	1.025	1.01	2.29	0.21E+05
86	1.00	0.00	0.84	0.259	0.312	0.765	0.284	1.41	2.08	0.41E+05
87	1.00	0.00	0.85	0.267	0.304	0.613	0.525	1.16	1.63	0.54E+05
88	1.00	0.00	0.83	0.258	0.301	0.542	0.498	1.03	1.44	0.65E+05
89	1.00	0.00	0.79	0.238	0.364	0.595	0.609	0.93	1.17	0.75E+05
90	1.00	0.00	0.76	0.224	0.477	0.700	0.472	0.83	0.82	0.89E+05
91	1.00	0.00	0.74	0.217	0.504	0.688	0.559	0.77	0.77	0.99E+05
92	1.00	0.00	0.72	0.205	0.526	0.692	0.411	0.74	0.65	0.11E+06
93	0.49	1.13	1.69	0.587	0.555	1.000	0.980	2.00	3.33	0.90E+05
94	0.49	1.13	2.14	0.696	0.370	0.810	0.434	2.26	3.95	0.19E+06
95	0.49	1.13	3.62	0.868	0.227	0.613	0.849	2.19	5.17	0.20E+06
96	0.34	2.05	2.54	0.764	0.401	0.899	0.104	3.10	5.77	0.12E+06
97	0.34	2.05	3.40	0.853	0.315	0.643	0.520	2.46	5.56	0.17E+06

98	0.34	2.05	2.90	0.814	0.354	0.714	0.423	4.00	5.30	0.15E+00
99	0.34	2.05	3.44	0.856	0.333	0.874	0.826	3.13	7.14	0.11E+00
100	0.34	2.05	3.18	0.835	0.364	0.924	0.537	3.16	6.82	0.11E+00
101	0.27	2.90	2.89	0.807	0.388	0.768	0.263	3.29	6.67	0.10E+00
102	0.27	2.90	3.31	0.846	0.339	0.591	0.330	2.70	6.00	0.11E+00
103	0.27	2.90	4.50	0.912	0.279	0.558	0.791	2.00	7.14	0.11E+00
104	0.27	2.90	5.07	0.928	0.259	0.539	0.172	2.54	7.50	0.15E+00
105	0.27	2.90	5.40	0.936	0.248	0.526	0.800	2.50	8.33	0.15E+00
106	0.27	2.90	2.83	0.801	0.427	0.735	0.196	2.88	6.00	0.12E+00
107	0.27	2.90	2.70	0.785	0.408	0.625	0.142	2.02	5.45	0.14E+00
108	0.27	2.90	2.09	0.686	0.507	0.860	0.360	3.22	5.60	0.10E+00
109	0.16	5.61	1.35	0.476	0.732	0.780	0.019	3.84	5.20	0.72E+05
110	0.16	5.61	1.77	0.610	0.670	0.673	0.105	3.42	5.20	0.80E+05
111	0.16	5.61	2.01	0.669	0.633	0.607	0.142	3.14	5.56	0.97E+05
112	0.16	5.61	1.92	0.649	0.645	0.650	0.210	3.34	5.36	0.89E+05
113	0.16	5.61	2.17	0.703	0.610	0.553	0.180	2.88	5.17	0.11E+00
114	0.16	5.61	2.42	0.745	0.561	0.485	0.200	2.04	4.70	0.13E+00
115	0.16	5.61	2.86	0.803	0.511	0.448	0.283	2.48	5.26	0.14E+00
116	0.16	5.61	3.26	0.842	0.470	0.436	0.229	2.44	5.50	0.14E+00
117	0.16	5.61	2.23	0.713	0.574	0.439	0.081	2.41	4.11	0.14E+00
118	0.16	5.61	1.91	0.647	0.630	0.615	0.029	3.24	5.17	0.93E+05
119	0.16	5.61	1.72	0.595	0.820	0.582	0.358	2.43	3.75	0.53E+05
120	0.16	5.61	2.40	0.742	0.654	0.406	0.259	1.90	4.17	0.70E+05
121	0.16	5.61	2.78	0.795	0.601	0.378	0.311	1.81	3.95	0.62E+05
122	0.16	5.61	2.86	0.803	0.576	0.309	0.597	1.52	3.26	0.11E+06

123	0.16	5.61	2.40	0.742	0.646	0.337	0.328	1.01	3.26	0.04F+05
124	0.16	5.61	2.32	0.729	0.641	0.268	0.246	1.36	2.34	0.11F+06
125	0.16	5.61	2.52	0.760	0.610	0.266	0.356	1.31	2.27	0.13F+06
126	0.27	2.90	2.18	0.703	0.552	0.489	0.562	1.05	3.11	0.04F+05
127	0.27	2.90	1.80	0.617	0.639	0.679	0.490	4.12	3.95	0.65F+05
128	0.27	2.90	2.10	0.688	0.525	0.396	0.454	1.43	2.78	0.12F+06
129	0.27	2.90	2.58	0.769	0.452	0.356	0.457	1.58	2.68	0.12F+06
130	0.27	2.90	2.96	0.814	0.396	0.314	0.672	1.30	2.78	0.13F+06
131	0.27	2.90	2.86	0.803	0.388	0.289	0.554	1.24	2.88	0.14E+06
132	0.27	2.90	3.23	0.840	0.356	0.278	0.577	1.22	2.73	0.15F+06
133	0.34	2.05	2.07	0.682	0.508	0.627	0.556	1.85	3.41	0.09F+05
134	0.34	2.05	2.94	0.812	0.355	0.418	0.860	1.52	3.75	0.11F+06
135	0.34	2.05	3.22	0.839	0.297	0.331	0.686	1.37	3.00	0.12F+06
136	0.34	2.05	2.15	0.698	0.472	0.412	0.552	1.29	2.50	0.14F+06
137	0.34	2.05	2.19	0.707	0.444	0.374	0.364	1.23	2.08	0.15F+06
138	0.34	2.05	1.73	0.599	0.540	0.414	0.372	1.21	1.88	0.15F+06
139	0.49	1.13	2.18	0.704	0.372	0.599	0.721	1.65	3.26	0.09F+05
140	0.49	1.13	2.74	0.789	0.296	0.468	0.711	1.47	3.13	0.11F+06
141	0.49	1.13	3.00	0.818	0.258	0.401	0.653	1.39	3.26	0.12F+06
142	0.49	1.13	2.76	0.792	0.252	0.357	0.571	1.31	3.00	0.13F+06
143	0.49	1.13	3.33	0.847	0.214	0.314	0.804	1.25	2.78	0.14F+06

EXPS. 144 TO 146 STAND FOR VELOCITY PROFILE ONLY.

APPENDIX II

The main part of the design of trench weirs includes that of Longitudinal Bar Bottom-Racks. The present study indicates that the following field parameters are required for the design of such racks :

- (i) The total stream flow , Q_S
- (ii) The diverted flow through the rack , Q_D
- (iii) The width of the rack /channel , B
- (iv) The depths , Y_0 and Y_{1e}
- and (v) The diameter of the bar , D and spacing , S between the bars.

The spacing can be chosen on the basis of the size of the sediment present in the stream.

With the suggested correlations one can use the above parameters to calculate the length of the rack. A simple Fortran Program has been developed and given on the next page. The length calculated from this program with the available data for BANU and PARAI trench weirs alongwith their recommended length is given in Table I

TABLE I Comparision of design lenth.

weirs	Length (m) calculated by present method	Length(m) provided
BANU	1.1	2.0
PARAI	1.5	2.0

PROGRAM RACK

TRENCH WEIR -- RACK DESIGN

THE FOLLOWING PROGRAM CALCULATES THE LENGTH(L1) OF A BOTTOM RACK FOR WHICH APPROACH FLOW(QS), DIVERTED FLOW(QD) THROUGH RACK, Y0, Y1e, DIAMETER(D) OF BARS, SPACING (S) BETWEEN THE BARS AND WIDTH(B) OF CHANNEL IS KNOWN. HERE Y0 IS DEPTH AT A DISTANCE '5Y1e' FROM U/S BRINK OF RACK & Y1e IS U/S BRINK DEPTH.

```
REAL L, L1
READ(21,*) QS,QD,Y0,Y1e,D,S,B
VO=QS/(B*Y0)
EO=Y0+((QS*QS)/(19.62*B*B*Y0*Y0))
EPS=(S/(D+S))
```

THE OPEN AREA RATIO "EPS" HAS BEEN MULTIPLIED BY 0.45 BY CONSIDERING 10% REDUCTION DUE TO FRAME WORK AND 50% DUE TO CLOGGING TO GET "EPS1".

```
EPS1=0.45*EPS
FO=QS/(B*3.132*(Y0**1.5))
YC=((QS*QS/B*B*9.81)**(1.0/3.0))
DS=D/S
IF ((Y0.GT.YC).AND.(Y1e.LT.YC)) GO TO 50
IF ((Y0.GT.YC).AND.(Y1e.GT.YC)) GO TO 100
CD=(ALOG(D/S)*0.36)-1.084*(VO*VO/(19.62*EO))+1.115
WRITE(22,7)
FORMAT(/,20X,'FLOW IS B1 TYPE')
WRITE(22,8)
FORMAT(/,20X,20('-'))
GO TO 150
CD=(ALOG(D/S)*0.20)-0.247*(VO*VO/(19.62*EO))+0.601
WRITE(22,10)
FORMAT(/,20X,'FLOW IS A1 TYPE')
WRITE(22,8)
GO TO 150
CD=(ALOG(D/S)*0.28)-((VO*VO/(19.62*EO))*0.565)+0.752
WRITE(22,15)
FORMAT(/,20X,'FLOW IS A3 TYPE')
WRITE(22,8)
GO TO 150
L=QD/(EPS1*B*CD*(SQRT(19.62*EO)))
```

LENGTH, L IS INCREASED BY 10% TO GET DESIGN LENGTH ,L1.

```
L1=1.1*L
WRITE(22,12) QS,QD,Y0,D,S,B,CD,DS,YC,Y1e,EO,FO,EPS,L
FORMAT(/,10X,'QS=',F7.3,'CUMECs',/,10X,'QD=',F7.3,'CUMECs',
1/,10X,'Y0=',F6.3,'METERS',/,10X,'D=',F6.4,'METERS',/,10X,
1/,10X,'S=',F6.4,'METERS',/,10X,'B=',F5.2,'METERS',/,10X,'CD=',F6.3,
1/,10X,'D/S=',F6.3,/,10X,'YC=',F6.3,'METERS',/,10X,'Y1e=',F6.3,
1METERS',/,10X,'EO=',F6.3,'MTRERS',
1/,10X,'FO=',F6.3,/,10X,'OPEN AREA RATIO=',F6.3,/,20X,'LENGTH OF
1 THE RACK RECOMMENDED=',F5.1,'METERS',/,20X,30('-'))
STOP
END
```